

Novel Optical Techniques to Enable Network Management in All-Optical Networks

TSE, Kam Hon

A Thesis Submitted in Partial Fulfillment
of the Requirements for the Degree of
Doctor of Philosophy
in
Information Engineering

The Chinese University of Hong Kong

August 2012

UMI Number: 3537662

All rights reserved

INFORMATION TO ALL USERS

The quality of this reproduction is dependent upon the quality of the copy submitted.

In the unlikely event that the author did not send a complete manuscript and there are missing pages, these will be noted. Also, if material had to be removed, a note will indicate the deletion.



UMI 3537662

Published by ProQuest LLC (2013). Copyright in the Dissertation held by the Author.

Microform Edition © ProQuest LLC.

All rights reserved. This work is protected against unauthorized copying under Title 17, United States Code



ProQuest LLC.
789 East Eisenhower Parkway
P.O. Box 1346
Ann Arbor, MI 48106 - 1346

Abstract

This thesis addresses three important network management aspects of optical networks, namely, optical lightpath tracing problem for all-optical networks, all-optical packet buffering in optical packet switching networks, power-efficient operation in wavelength division multiplexing passive optical networks (WDM-PON).

Lightpath tracing through all-optical encoder

In an all-optical reconfigurable wavelength routing network, the lightpath of the optical data packets can be reconfigured, via the optical cross connects (OXC) residing at each network node. In order to monitor any possible routing errors, any possible causes of signal quality degradation, detect any source of malicious or attack traffic and provide quality of service (QoS) aware next-hop routing strategy, monitoring of lightpath of optical data packets is necessary. This scheme encodes the lightpath information into the label of individual optical packet. Each network node is assigned with a distinct prime number as an identification tag. By using the optical encoders located at the outputs of OXCs, the label value of the packets will be multiplied by the prime number designated to the respective OXC, residing at the network node. Hence, the information of the network nodes that the packet has traversed will be encoded to the label as the product of all the prime numbers assigned to all traversed network nodes.

Therefore, at the destination node, the whole physical lightpath of each received optical data packet can be easily identified through factorization of the encoded label value.

Our scheme provides substantial reduction in the requirement of fiber delay lines, as compared to the time-delay recognition techniques. It offers fast detection when comparing with pilot tone detection method. Besides, possible network looping problem can be detected and the encoded label can be acted as time-to-live (TTL) identifier of the optical packet.

All-optical power-controlled optical packet buffer

All-optical packet buffer is essential for the contention resolution in all-optical packet switching network. In order to realize simple and efficient operation of optical packet buffer, we propose the use of all-optical power-controlled packet buffer for which the number of circulating loops is controlled by the input signal power (i.e. input signal with higher power will experience longer delay). We formulate the problem of designing a re-circulating delay buffer into signal power dependent filtering problem. The optical OOK signal first passes through a re-circulating loop generating multiple copies at different time instants that each delayed copy will have halved power as the previous one. Then it will pass through the signal power dependent filter implemented by using optical nonlinear effect. The filter has the characteristics that only signal (packet copy) with specific power level can be outputted while the others get attenuated and

therefore cleared. As a result, in order to change the amount of delay, we just need to change the input signal power such that the signal with specific delay will fall into the pass band of the power dependent filter and get outputted.

Compared with other delay schemes which use many SOAs as gates to control the number of re-circulating delay or implementing tunable wavelength converter and passes through wavelength dependent delay, our scheme provides easy control of the delay required.

Signaling techniques for power-efficient operation of WDM-PON

In WDM-PON, the upstream signal at the optical network unit (ONU) can be generated by re-modulating the downstream signal received from the optical line terminal (OLT). However, the conventional architecture may suffer from power consumption problem. When there is no downstream signal, the ONU is not able to send any upstream data. Thus even if there is no traffic on the line, the OLT has to send the downstream signal continuously, in order to ensure the ONU can always be able to send its upstream data. In such networks, burst-mode traffic transmission can provide improvement on power efficiency. We propose a signaling technique to send “Wake Up” message from the ONU to OLT, to notify the transceiver of the OLT to recover from sleep mode. It is done by modulating the Amplified Spontaneous Emission (ASE) noise in RSOA at the ONU with the particular ONU specific pilot tone monitoring signal. Thus, it does not require the presence of the remodulating downstream signal. At the OLT, a specific module

is needed for the detection of the pilot tones from different ONUs and then activate the corresponding transceiver. Our scheme offers simple and cost-effective approach for power-efficient operation in the WDM-PON.

簡要

這篇論文討論了三個重要的全光網絡的網絡管理方向，分別為在全光封包交換網絡的光路追蹤問題，光封包的暫存及在波分複用無源光網絡（WDM-PON）的能源節省運作。

使用全光編碼器進行光路追蹤

在所有全光封包交換網絡中，數據包的路由光路是可以被通過光學交叉連接（OXC）的網絡節點重新配置。要監控任何可能的路由錯誤、信號質量下降的任何可能的原因、發現任何惡意或攻擊流量的來源、或提供服務質量（QoS）的路由策略，光學數據包的光路監測是必要的。此方案編碼光路信息到光學數據的標籤，每個網絡節點被分配一個獨特的質數為識別標記的光路信息。使用位於 OXC 輸出端的光學編碼器，每次當數據包通過該網絡節點時，數據包的標籤值將乘以特定的質數。網絡數據包已經走過的節點將被編碼的標籤為代表的網絡節點的所有素數的乘積。因此，在標籤的檢示器中，光數據包走過的每個網絡節點都可以很容易地通過標籤值的因式分解求得。

相比使用時間延遲識別技術，我們的設計大幅減少了光纖線的長度要求。此外，與導頻訊號檢測方法相比，它提供了快速檢測的好處。此外，網

絡循環的問題也可以檢測。編碼標籤也可以作為的光封包的保存週期指示器 (TTL)。

功率控制的全光封包緩衝器

全光封包緩衝區全光交換網絡中是非常重要的。為了實現簡單而有效的光學數據包緩衝操作，我們提出使用功率控制時間延遲的全光數據包緩衝區。的循環迴路的數量是由輸入信號的功率控制（即具有較高的功率輸入信號將經歷更長的時間延遲）。我們把循環延遲緩衝器重新設計成信號功率依賴過濾的問題。光信號首先通過在不同的時刻，每延遲副本將減半功率與前一個通過循環生成多個副本的循環。然後，它會通過信號的功率大小而使用非線性光學效應來實施過濾。過濾器只與特定功率水平的信號，可以輸出，而別人得到減毒，因此清除的特點。因此，為了改變延遲量，我們只需要改變輸入信號功率等具體延遲的信號，將陷入電源依賴的濾波器的通帶和輸出。

比起使用許多的 SOA 來控制循環延遲或使用可調諧波長轉換器及波長依賴時滯的方案，我們的計劃提供更容易的延遲控制。

信號電源效率的 WDM-PON 的操作技巧

在 WDM-PON 中，光網絡單元 (ONU) 的上傳信號通過對由光線路終端 (OLT) 的下傳信號的重新編寫產生。傳統上，這設計產生功耗的問題。

例如：如果沒有下傳信號，光網絡單元不能發送上傳數據。因此，即使沒有數據傳送，光線路終端也要不斷傳送下傳信號，爲了確保光網絡單元總是能夠發送上傳數據。在這種網絡中，突發傳送模式可以提供電源效率上的節省。我們提出了一個信號傳送技術來由光網絡單元向光線路終端發送“喚醒”消息，以通知光線路終端的收發器從睡眠模式恢復。這技術是通過對在 RSOA 放大自發輻射（ASE）噪聲進行特定導頻信號的，因而不需要重新調制下游信號。在光線路終端，額外的模塊將負責檢測不同光網絡單元的導頻信號，然後啓動相應的收發器。我們的計劃提供了在 WDM-PON 的簡單和高成本效益的能源節省方案。

Acknowledgements

First, I would really like to thank my thesis supervisor Prof. Chun-Kit Chan, Calvin for his constant guidance, tremendous support and encouragement during my PhD study. His knowledge, hard work, dedication to excellence and careful attention to details, have driven the process of this thesis. The insightful discussions and invaluable reviews were of great benefits to my research experience. It has been an enlightening experience for me to do my research work under his extraordinary supervision.

I am grateful to Prof. Lian-Kuan Chen for his valuable comments, fruitful discussions and enormous support on my research's works and studies. His in-depth knowledge and the strong sense of direction have always been inspirational to me.

It is my pleasure to work with a group of talented students and research staffs in Lightwave Communications Lab in the Department of Information Engineering, CUHK, including Jordan Tse, Zhenchang Xie, Dr. Ming Li, Jonathan Chong, Yang Qiu, Jing Xu, Shuqiang Zhang, Dong Shen, Wei Jia, Pulan Li, Zhixin Liu, Francis Yuen, Qike Wang, Hon-Tong Luk. I wish to express my thanks to Alex Siu and Barry Kwok for their help in electronics hardware implementations.

My sincere gratitude is extended to Eric Ho for his unfailing friendship, encouragement, and fatherly mentorship, both in my life and in my study.

Finally, I am deeply indebted to my family and I would like to dedicate this thesis to my God for his agape love.

Table of Contents

Abstract	i
Acknowledgements	viii
Chapter 1 Background	1
1.1 <i>All-Optical Packet Switching Networks</i>	3
1.1.1 <i>Packet Buffering</i>	4
1.1.2 <i>Route Tracing</i>	7
1.2 <i>Wavelength Division Multiplexing Passive Optical Networks (WDM-PON)</i>	12
1.2.1 <i>ONU Upstream Re-Modulation in WDM-PON</i>	12
1.2.2 <i>Green Networking</i>	13
1.3 <i>Contributions</i>	17
1.3.1 <i>Path Tracing Scheme for All-Optical Packet-Switched Networks</i>	17
1.3.2 <i>All-Optical Power-Controlled Optical Packet Buffer for All-Optical Packet-Switched Networks</i>	18
1.3.3 <i>Signaling Techniques for Power-Efficient Operation of WDM-PON</i>	19
1.4 <i>Organization of Thesis</i>	19
Chapter 2 Path Tracing Scheme for All-Optical Packet-Switched Networks	21
2.1 <i>Introduction</i>	21
2.2 <i>Path Tracing Using Prime-Number Tags</i>	26
2.2.1 <i>Network Node Tracing</i>	26
2.2.2 <i>Network Link Tracing</i>	28
2.2.3 <i>Network Looping Problem</i>	29
2.3 <i>Optical Implementation</i>	30
2.4 <i>Experimental Results</i>	38
2.5 <i>Multi-Level Amplitudes Of The Label</i>	41
2.6 <i>Required Maximum Fiber Delay</i>	44
2.7 <i>Summary</i>	47
Chapter 3 A Novel Fiber-based Variable All-Optical Packet Buffer based on Self-Phase Modulation Induced Spectral Broadening	48
3.1 <i>Introduction</i>	48
3.2 <i>Input signal power dependent delay</i>	51
3.3 <i>Numerical Simulation Studies</i>	54

3.4	<i>Experimental Results</i>	64
3.5	<i>Discussion</i>	68
3.6	<i>Summary</i>	71
Chapter 4 A Cost-effective Pilot-Tone-based Monitoring Technique for Power Saving in RSOA-based WDM-PON		73
4.1	<i>Introduction</i>	73
4.2	<i>Proposed System Architecture</i>	75
4.3	<i>Experimental Setup and Result</i>	78
4.4	<i>Power Saving Efficiency Calculation</i>	82
4.5	<i>Summary</i>	86
Chapter 5 Conclusions and Future Work		87
5.1	<i>Conclusions</i>	87
5.2	<i>Future Work</i>	88
Bibliography		90
Publications during PhD Study		98

Chapter 1 Background

Today, Internet is rapidly developed to meet the huge demand of fast information exchange and bandwidth-intensive networking services. With the Internet, users around the globe can enjoy the applications like web surfing, video streaming, file sharing, video conferencing, online gaming, etc. To support such long distance and high data rate Internet traffic, fiber optics communication is essential with its advantages of huge bandwidth capacity, low signal attenuation and impairments when the light signal is transmitting through optical fiber.

To fully utilize the potential bandwidth of the optical fiber, wavelength division multiplexing (WDM) technique is considered as a best candidate that allows multiple optical signals at different wavelengths to transmit along a single piece of optical fiber, simultaneously. It provides easy multiplexing or de-multiplexing of the different optical signals, via passive optical filter, without requiring any timing synchronization when comparing with the conventional time division multiplexing (TDM) technique. Moreover, in the existing WDM link, WDM channels can be added easily with the increasing traffic demand. The WDM multiplexer or de-multiplexer can be made using arrayed waveguide grating (AWG) technology which offers low cost and high port count advantages. As a result, it is a key building block in wavelength-division-multiplexing passive optical network. The spectral response of such AWG devices is temperature sensitive. Any spectral misalignment between the signal wavelength and the AWG's passband may induce severe signal degradation to the WDM channels.

Nevertheless, athermal AWG is available to assure temperature stability and maintain stable filtering channel outputs, with any active temperature control circuits. Besides AWG, fiber Bragg gratings and thin film coating interference filters are also commonly employed as channel (wavelength) add-drop filters. Nowadays, WDM standards are classified as coarse WDM (CWDM) and dense WDM (DWDM) with 20-nm and 0.8-nm (100-GHz @1550nm) channel spacing respectively.

Today's telecom network comprises three kinds of sub-networks, namely access (spanning about 1 to 10 km), metropolitan (covering about 10 to 100 km), and long haul (extending to 100s or 1000s of km) [1] networks. They form a hierarchical structure that links between the end users and the core servers in the Internet.

Within these optical sub-networks, optical signals can be transmitted transparently without any intermediate optical-electrical-optical (O-E-O) conversion. They offer the advantages of modulation format transparency, bit-rate transparency and protocol transparency. The intermediate O-E-O conversion is costly and difficult to be upgraded to higher bit rate, therefore should be avoided. As O-E-O conversion is typically operated in a channel by channel manner, the required number of O-E-O conversion modules would increase with the number of WDM channels. The network is referred as all-optical network or transparent network if all the nodes on the network are equipped with all-optical cross connects (OXC) or reconfigurable optical add-drop multiplexer (ROADM) without any electronic regeneration function nor O-E-O conversion.

In this chapter, we will introduce some promising all-optical WDM network architectures in access and core network. We will also discuss some important problems in these WDM networks and their previously reported solutions.

1.1 All-Optical Packet Switching Networks

In a core network, the network nodes with OXCs are connected in mesh topology through optical fibers. To achieve good flexibility and fine granularity on routing and switching of the optical signals inside optical network, optical packet switching (OPS) is proposed as a long term core network switching technology. In OPS network, each network node consists of an optical packet switch that performs packet synchronization, packet switching and packet header processing functionalities. For all-optical packet switching networks, optical packets are transmitted transparently through the OXCs inside the network without O-E-O conversion. In such network, as each network node is required to perform packet processing all-optically, many new all-optical packet processing techniques have been proposed. In the following discussion, we will focus on the all-optical packet processing techniques for packet buffering and packet route tracing.

1.1.1 Packet Buffering

In an all-optical OPS network, the optical packets have variable packet lengths and are transmitted asynchronously. The routing decision made at each network node is based on its current traffic loading and the destinations of the received data packets. The decentralized approach of the packet switching and routing decision will increase the packet-contention-probability when comparing with optical circuit switching. Packet contention occurs when two or more packets try to leave the switch from the same output port of an OXC at the same time. To solve such a conflict, contention resolution is needed for optical packets in order to reduce the packet-loss rate and therefore increases the optical network throughput.

In electronic routers, contention is usually resolved by a store-and-forward technique, which means that the packets in contention are stored in a queue and are sent out one by one. This is possible because of the available electrical random access memory (RAM). In an all-optical packet switch, we have to take a different approach because there is no ready-to-use optical RAM [2].

To solve packet contention, one of the optical packets may be transferred into different time, different space or different wavelength. For solving packet contention in time domain, the optical packets can be stored in optical delay lines, in order to resolve the contention of optical packets at the output ports of the OXCs. The optical delay lines can be fixed or reconfigurable that the delay time of the optical packet inside the optical delay line can be altered. On the other hand,

deflection routing can also be a contention resolution method such that one packet is forwarded to the desired output port, while the other packets are routed to other links which may have longer propagation delay. This method resolves packet contention in space domain. The third method is by employing all-optical wavelength conversion techniques, in which one of the contented packets will have its wavelength converted. Thus both of the optical signals will be forwarded to the same output port on different wavelengths and therefore resolves the contention problem [2].

There are different categories of optical delay lines, including continuously tunable ones or discretely variable ones. For continuously tunable category, it can be implemented by wavelength conversion followed by a dispersive medium with group velocity dispersion (GVD) [3]-[8]. The GVD mediums can be dispersion compensating fiber (DCF) [3], [4] and linearly chirped fiber Bragg grating [5]. As the signal on different wavelengths will experience different propagation delays when being transmitting in dispersive medium, by changing the wavelength of the input signal, the delay can be adjusted accordingly. Although the delay of linearly chirped fiber Bragg grating can be changed by optical pumping [6] and temperature control [7], the use of linearly fiber Bragg grating can only provide small tunable delay range which limits its use for specific applications like beamforming system for phased array antennas. Another kind of optical delay line is based on slow light technique. Slow light technique is usually achieved with resonant effects that cause large normal dispersion in a narrow spectral region, which increases the group index, thus

reduces the group velocity of optical pulses. As a result, the propagation time of the packet inside the optical fiber will be changed. Optical resonances associated with stimulated Brillouin scattering (SBS) [9],[10], stimulated Raman scattering [11], and parametric amplification [12] in optical fibers have been recently demonstrated to achieve slow light technique. Nevertheless, their applications might be limited by the small amount of induced delay, delay tuning speed limited by wavelength conversion tuning speed and the possible severe signal degradation or attenuation at increased delay values. The different approaches of the optical buffering always have benefits and drawbacks in terms of maximum delay, accuracy of delay, wavelength of operation, speed of operation, pulse distortion, and conceptual complexity [3].

Considering the application of optical packet buffer, it will require the feature of a long maximum delay with fast speed of operation. Discrete delay operation employing wavelength conversion for optical packet buffering is proposed in [8]. A common way to implement optical buffers are based on an optical re-circulating loop, which requires all-optical switches [13], optical switching via semiconductor optical amplifiers (SOAs) [14], [15], or through nonlinear polarization rotation inside the SOA [16], to control the number of circulations for the optical packet. However, it requires synchronization between the switching time and the cycle of the packet propagation. In [17], an optical re-circulating loop with an optical thresholding function is used to control the propagation of low-priority signal inside the loop, via wavelength conversion, so as to resolve the contention. In [18], the signal's wavelength is shifted by a certain

amount after each cycle of circulation in an optical re-circulating loop; the signal will be outputted from the re-circulating loop when its wavelength is shifted to the center of the output filter. Thus, the signal's delay could be varied and controlled by changing the input signal's wavelength.

1.1.2 Route Tracing

Besides packet contention problem, all-optical OPS networks require more complicated network management compared with optical circuit switching networks, as there is still lack of route tracing methods in the OPS network. In optical circuit switching network, lightpath from the source to destination node is already established before the signal started to transmit. As a result, failure across the lightpath is easily detected during connection establishment stage. However, in optical packet switching network, the physical routing path of the packet is still unknown before packet transmission. And it is the intermediate nodes that determine the actual physical routing path of the packet. With the route tracing information of the packets, network operators can easily diagnosis the possible sources of failures, which may include fiber cut, signal degradation, routing failure, etc [19]. When a failure occurs, we can trace it from that packet's routing path. For example, when there is a routing failure occurred at the intermediate network node, we can retrieve the information of the failed network node from its wrongly routed path. When there is a network link which causes signal degradation, we can observe the paths of all signal degraded packets. The

common link from all those paths gives a good estimation of the link which causes signal degradation. When there is a fiber cut occur, we can no longer retrieve the packets' routing paths which contain the disconnected network link. Moreover, when there exists any malicious or attack traffic, it will be useful to trace down the source of the attack through examining and analyzing the path information of the received packets [20].

Besides failure diagnosis, route information of the packets can also enhance quality of service (QoS) functionality. If path tracing is performed at certain strategic nodes in the network, the traced path information on the previously traversed network nodes or links of the data packets could be used to deduce the actual or relative amount of accumulated optical impairments or temporal delay suffered by the dynamically routed data packets. Such information is beneficial to estimate the signal quality, and make strategic scheduling and routing decisions to meet the quality of service (QoS) requirement of the network. For instance, the priorities of the next-hop routing paths of an optical data packet at the OXC can be re-adjusted according to its estimated previous path.

To perform path tracing in all-optical fully-reconfigurable OPS network which the packets are transmitted transparently throughout the network, the route information is undetermined at the source network nodes and the route information is difficult to be added to the headers of packets in the intermediate network nodes because the packets pass through the intermediate nodes without O-E-O conversion. Therefore, it is highly desirable to have optical techniques to

perform such physical path tracing on the optical layer so as to realize connection management in an optical packet-switched network in a more efficient way.

Recently, several schemes, based on pilot-tones identification [21],[22] and time-delay recognition [23]-[26], have been proposed to monitor the connections within an OXC or a cascade of OXCs. Regarding to the pilot-tone identification schemes [21],[22], a pilot tone at a distinct frequency is added to each input port of the OXC, as the input port identifier. By examining the pilot tone frequencies contained in the switched optical signal at each output port of the OXC, the switching connections of the OXC could be derived. This scheme could be further extended to realize path tracing in an all-optical WDM packet-switched network. A pilot-tone at a distinct frequency is assigned to each network node as node identifier, which is added to every optical signal that has traversed through that node. Different optical signals routed into different network nodes will be injected with pilot-tones at different frequencies. The receiving node can then identify which network nodes the optical signal has passed through by examining the presence of various pilot-tones. However, this scheme suffers from slow monitoring through the use of low frequency pilot-tones.

Regarding to the time-delay recognition schemes [23]-[26], the optical pulses at different input or output ports in an OXC would experience different time delays, via some delay circuits. Hence, by examining the unique temporal pulse patterns generated, the connection states between the input and the output ports of the OXC could be derived. The scheme could be further extended to realize path monitoring by assigning different time delay patterns to different

network nodes. However, the scheme suffers from poor scalability, in terms of the amount of fiber delay required at each node in order to avoid any ambiguity among different possible paths. Besides, precise synchronization is needed in order to retrieve the correct pulse positions of the delay patterns.

Lightpath tracing is also proposed to optical circuit switching network to facilitate network management function including fault isolation [27]. In such network, as the signal's path is determined before it is transmitting inside the established signal, therefore, path-ID can be injected into the signal at the source node. At the intermediate node, low cost path-ID detectors are employed to monitor the path of the incoming signals. The path-ID labeling can be implemented by using AM pilot-tone [27], [28] or non-AM labeling techniques [29]-[31]. AM pilot-tone technique suffers from large crosstalk to the data channel in DWDM amplified transmission because of cross-gain modulation in optical amplifiers and/or stimulated Raman scattering (SRS) in the fiber [31]. The non-AM labeling techniques include frequency shift keying [29], [30], in-band frequency modulated (FM) tone [31]. Those techniques can introduce complexity to the system implementation.

To support multiple labels detection at the intermediate network node with a single label monitor, another lightpath labeling scheme based on constant weight code label encoding [32], [33] has also been recently proposed. It is realized by embedding the label or low-speed data, which contains lightpath identification information, to the data signal by means of a complementary constant-weight code (CCWC). Electrical direct sequence code-division-

multiple-access (CDMA) technique is employed to support simultaneous reception of multiple labels from different WDM signals, via single low-speed photo-detector. However, the CCWC technique would impose redundancy on the original data and violate data format transparency. In addition, lightpath tracing or routing failure detection is performed at the intermediate network node. Moreover, this scheme is suitable for the circuit switching network, in which the routes of the packets are predetermined at the ingress node and all the intermediate nodes notify the mapping of the packet's routing path and its identification tag. Similar techniques have been proposed to introduce lightpath labeling to the signals in differential phase shift-keying (DPSK) [34], dual polarization-differential quadrature phase shift-keying (DQPSK) [35] and optical orthogonal frequency division multiplexing (OFDM) [36] formats.

1.2 Wavelength-Division-Multiplexing Passive Optical Networks (WDM-PON)

The wavelength-division-multiplexed passive optical network (WDM-PON) is a promising technology for the next-generation access networks. In WDM-PON, each user or optical network unit (ONU) will have a dedicated wavelength channel to communicate with the optical line terminal (OLT) and an arrayed waveguide grating (AWG) router is used to distribute the signals from the OLT to different users. As a result, it provides high data capacity, privacy, and protocol transparency as compared with conventional time-division-multiplexing passive optical network (TDM-PON).

1.2.1 ONU Upstream Re-Modulation in WDM-PON

In conventional WDM-PON system, as each user communicate with the OLT in dedicated wavelength channel, therefore, at the OLT, it will have an array of laser modules with different center wavelengths to generate downstream signals to the ONUs. Moreover, at each ONU module, the laser at specific center wavelength is employed in order to send the upstream signal to the OLT and this introduces the need of wavelength specific ONU modules. There is a need of low-cost colorless optical sources at the ONUs in order to reduce the high deployment cost of WDM-PON, compared with TDM-PON in which the wavelength specific ONU introduces significant challenges in managing production lines, inventory stocks, sparing, and maintenance [37].

Data re-modulation of downstream signal for the upstream signal at the ONU can be a technique for the realization of colorless ONU transponder. This technique replaces the use of wavelength specific laser into colorless re-modulator at the ONU module. Several re-modulation schemes have been proposed, including using both downstream and upstream on-off keying (OOK) [38]; downstream differential phase shift keying (DPSK) and upstream OOK [39]; downstream inverse return-to-zero (IRZ) and upstream OOK [40]; downstream low extinction-ratio (ER) OOK and upstream DPSK [41]. Recently, re-modulation scheme using reflective semiconductor optical amplifier (RSOA) at the ONU has recently been proposed with the advantages of potentially low cost and relatively high data rate [42]. In addition, 10-Gb/s operation has been demonstrated using RSOA [43].

1.2.2 Green Networking

Recently, there has been an increasing attention to power consumption saving in many fields. In information and communication technology (ICT), it is estimated that access network consumes around 70% of overall telecom network energy consumption [44] due to the presence of huge number of active devices. In addition, an estimation shows that access networking equipments are less than 15% utilized [44] and large portion of energy is therefore consumed by the idle devices, as the networks are engineered for satisfying the peak traffic load

requirement. Hence, reducing energy consumption in access networks during off-peak hours can lead to major saving in Internet energy consumption.

From [45], it was stated that the number of active network subscribers during the period between 0200 and 0800 are much less than that between 1700 and 2200. Moreover, WDM-PON can be integrated with wireless-mesh network as fiber-wireless (FiWi) architecture where multiple ONUs serve as gateways of a whole wireless-mesh network, similar to WOBAN [44] which combines the advantages of both optical and wireless communications. The multipath divergence characteristic of this architecture provides load balancing and failure restoration features.

In WDM-PON, energy saving can be an important issue due to the huge number of ONUs in the network. While the network usage from the network subscribers is time-varying at different periods within a day, the ONUs do not need to operate continuously for a whole day. As a result, when there are network subscribers who do not have active data transmission during off-peak hours, the transponders in the ONU and the corresponding modules at the OLT can be turned off for power saving purpose. However, there is a problem when the transponders in the OLT are turned off. When the network subscribers have traffic demand, the OLT can't receive the requests to activate the corresponding modules for data communication. Moreover, when the ONUs are operating in upstream re-modulation manner, the ONU can't send the upstream signal without having received downstream signal from the OLT. Therefore, in order to ensure that the ONU can send upstream signal to the OLT, the OLT has to send the downstream

signal at all times and this will inhibit the power saving operation at the OLT [46]. To enable the OLT and the ONUs with the power saving operation (i.e. the ONUs' and the OLT's transponders can be turned off when the ONUs do not have traffic demand), certain signaling technique should be employed such that the ONUs can send data transmission requests to the OLT when the corresponding transponders have turned into power saving mode, for notifying the OLT to activate the corresponding transponders for data transmission.

In [46], a power saving scheme for WDM-PONs with colorless ONUs was proposed by using a wavelength tunable laser to poll individual ONUs in the network periodically. Their upstream transmission requests are monitored by employing a monitor with a wavelength tunable filter to extract the requests from the ONUs at different wavelengths sequentially. Thus, the optical channel at the OLT can be turned off to save power, when there is no active data in both downstream and upstream directions, simultaneously. However, the deployment of the wavelength tunable transceiver for the monitor can be costly. In addition, the OLT's channels wake-up speed will depend on the wavelength tuning speed of the transceiver in the monitor and the number of ONUs in the power saving mode currently.

The work in [47] generates continuous light-emitting-diode (LED) based monitoring signal at the OLT and the colorless ONUs can re-modulate the downstream spectrum-sliced LED monitoring signal with an ONU-specific pilot tone signal and transmit back to the OLT. At the monitor of the OLT, it will detect the summation of all of the monitoring signals from all ONUs. The

detected signal will then be examined to extract the specific pilot tone signals from the ONUs. The presence of the pilot tone signal will indicate the specific ONU request to initiate data transmission. As LED's signal is broadband, therefore, only a single LED device at the OLT is needed to generate the downstream monitoring signal to the entire ONUs. In addition, only a single monitoring device is needed to detect all of the pilot tone signals from the ONUs. However, this scheme suffers from data transmission penalty, as the continuous LED signal from the OLT is broadcasted to the entire ONUs by spectrum slicing at the remote node of the WDM-PON. All ONUs receive the LED signal in addition to the OLT's downstream data signal. Although the spectrum sliced LED signal is relatively low in power as compared with the downstream data signal, it may cause beating noise to the downstream signal and its re-modulating upstream signal, thus degrades the downstream and the upstream data signals.

1.3 Contributions

1.3.1 Path Tracing Scheme for All-Optical Packet-Switched Networks

Among the potential techniques to achieve path tracing in all-optical packet-switched network, the pilot-tones identification suffers from slow monitoring through the use of low frequency pilot-tones and the time-delay recognition schemes suffers from poor scalability, in terms of the amount of fiber delay. Moreover, precise synchronization is required. On the other hand, the technique of CCWC coding of the data payload will impose redundancy on the original data and violate data format transparency.

We have proposed a novel optical encoding scheme to realize path tracing in optical network. A distinct prime number is assigned as the path information tag for each network node. Through employing optical label encoders based on prime number multiplication at the outputs of the network nodes, path information tag is embedded to the optical packet label. All the path information tags carried by the optical data packet are easily extracted and identified by simple computation on the optical packet label at the receiving node. The all-optical label encoder can manipulate the label on-the-fly and can support multi-wavelength's labels encoding operations, simultaneously. In addition, it is a passive device which favors green photonics processing at the intermediate network nodes. Besides, any possible network looping problem in the optical network could also be identified.

1.3.2 All-Optical Power-Controlled Optical Packet Buffer for All-Optical Packet-Switched Networks

As mentioned above, the techniques using wavelength conversion followed by dispersive medium and the slow light can only introduce small amount of delay. On the other hand, the demonstrations of all-optical recirculating loop for implementing buffer require complex control of the amount of delay of the optical packet signal inside the buffer.

We have proposed a novel all-fiber variable optical packet buffer, in which the amount of delay is controlled simply by adjusting the input signal power level. The higher the input signal power, the more number of the circulations of the signal looped through and hence more delay it experiences. In such case, the signal power at the buffer's output will not change regardless of the amount of delay. The delay control is based on self-cloning the input optical signal, followed by optical power dependent filtering. The suggested optical subsystem implementation comprises a passive optical delay loop circuit and two stages of self-phase modulation (SPM) in highly nonlinear fiber (HNLF), followed by offset filtering. Due to the intrinsic nature of SPM, it does not require polarization control and no additional laser source is required.

1.3.3 Signaling Techniques for Power-Efficient Operation of WDM-PON

As discussed above, the polling scheme of a tunable supervisory transceiver requires a costly transmitter and receiver at the OLT. On the other hand, the LED based monitoring signal scheme will suffer from downstream and upstream data transmission penalty for the normal operating ONUs.

To provide simple energy saving scheme without causing penalty to data transmission, we have proposed a simple and cost-effective signal monitoring scheme supporting power saving mode in WDM-PON. At the ONU, a low cost RSOA is employed in order to provide upstream signal re-modulation and amplification simultaneously. By modulating the amplified spontaneous emission (ASE) spectrum in RSOA at the ONU with the ONU-specific pilot tone monitoring signal, “wake-up” message can be sent to the OLT without the need of the presence of downstream signal, tunable supervisory transceiver or any dedicated light sources. Moreover, no additional penalty is introduced to the data transmission when the ONUs are operating in the normal data transmission mode.

1.4 Organization of Thesis

Chapter 2 presents the path tracing scheme in all-optical packet switched network through the use of all-optical label encoder to insert the path labels to the packets at the intermediate nodes. The feasibility of the label encoding

scheme is studied with experimental demonstration of the proposed optical encoder, the multi-level property of the optical packet label and the comparison of the maximum fiber delay required in the proposed scheme with the previously proposed approaches.

Chapter 3 presents a novel optical delay control mechanism to realize variable all-optical packet buffering. The packet buffer is implemented through the fiber-based device which consists of a passive fiber delay loop followed by an optical power dependent filter. The optical power dependent filter is realized by means of two stages of self phase-modulation-induced spectral broadening and offset filtering. The numerical simulation and experiment results are also presented.

Chapter 4 presents a simple and cost-effective signal monitoring scheme supporting power saving mode in WDM-PON. By modulating the amplified spontaneous emission (ASE) spectrum in RSOA at the ONU with the pilot tone monitoring signal, “wake-up” message can be sent to the OLT. The power saving operations of the ONU are demonstrated through experimental results. In addition, power saving efficiency of the proposed scheme is discussed.

Chapter 5 concludes this thesis and suggests the possible future research topics.

Chapter 2 Path Tracing Scheme for All-Optical Packet-Switched Networks

In this chapter, we propose a novel optical scheme to perform path tracing in an all-optical packet-switched network. Prime-number-encoded tag is employed as the distinct network node or network link identifier. As the optical data packet traverses every network node, the path trace is recorded and updated optically, through prime number multiplication via an optical delay circuit encoder. Hence, all traversed network nodes along the path of a received optical data packet can be retrieved and identified at the destination node, via simple prime number factorization. Possible looping of optical data packets in the network can also be detected. The scheme can facilitate the connection management in an optical packet-switched network.

2.1 Introduction

In an all-optical wavelength-division multiplexing (WDM) packet-switching network, the optical data packets can be flexibly routed, such that each optical data packet, being carried on the same or different wavelength carrier from the same source network node, can be delivered to different destination network nodes at different times. The routing decision made at each network node is based on its current traffic loading and the destinations of the data packets received. When an optical data packet arrives at a network node, its packet header, which is usually of lower data rate, is first extracted and detected,

so as to retrieve its destination address. The high-speed packet payload portion is buffered through fiber delay lines, before the optical packet is being switched, via the optical cross-connect (OXC), based on the routing decision made.

In order to assure reliable data delivery over high-capacity WDM networks, robust network management is indispensable. All the data paths in the network should be well-managed and monitored. During the traversal over the network, the optical data packets may possibly be routed to other wrong or alternative output ports of OXCs at the network nodes, due to the possible routing errors or malfunctioning of the switching modules in the respective OXCs. Hence, upon reception of the optical data packets at the destination node, identification of the exact physical network nodes or fiber links that the received optical data packets have actually traversed is very useful to derive and estimate its complete actual physical path. Such information is very useful to detect any possible network routing error due to possible malfunction of the reconfigurable optical routing devices, and diagnose the possible causes of signal quality degradation in the received optical data packets, by examining the optical impairments along the retrieved path.

Moreover, when there exists any malicious or attack traffic, it will be useful to trace down the source of the attack through examining the path information of the received packets. In addition, if path tracing is performed at certain strategic nodes in the network, the traced path information on the previously traversed network nodes or links of the data packets could be used to deduce the actual or relative amount of accumulated optical impairments or

temporal delay suffered by the dynamically routed data packets. Such information is beneficial to estimate the signal quality, and make strategic scheduling and routing decisions to meet the quality of service (QoS) requirement of the network. For instance, the priority or the next-hop routing path of an optical data packet at the OXC can be re-adjusted according to its estimated previous path. Besides, possible looping of the data packets in the network can be detected and the excessively looped packets will be discarded. In general, it is highly desirable to have optical techniques to perform such physical path tracing on the optical layer so as to realize connection management in an optical packet-switched network in a more efficient way.

Recently, several schemes, based on pilot-tones identification [21],[22] and time-delay recognition [23]-[26], have been proposed to monitor the connections within an OXC or a cascade of OXCs. Regarding to the pilot-tone identification schemes [21],[22], a pilot tone at a distinct frequency was added to each input port of the OXC, as the input port identifier. By examining the pilot tone frequencies contained in the switched optical signal at each output port of the OXC, the switching connections of the OXC could be derived. This scheme could be further extended to realize path tracing in an all-optical WDM packet-switched network. A pilot-tone at a distinct frequency is assigned to each network node as node identifier, which is added to every optical signal that has traversed through that node. Different optical signals routed into different network nodes will be injected with pilot-tones at different frequencies. The receiving node can then identify which network nodes the optical signal has

passed through by examining the presence of various pilot-tones. However, this scheme suffers from slow monitoring through the use of low frequency pilot-tones.

Regarding to the time-delay recognition schemes [23]-[26], the optical pulses at different input or output ports in an OXC would experience different time delays, via some delay circuits. Hence, by examining the unique temporal pulse patterns generated, the connection states between the input and the output ports of the OXC could be derived. The scheme could be further extended to realize path monitoring by assigning different time delay patterns to different network nodes. However, the scheme suffers from poor scalability, in terms of the amount of fiber delay required at each node in order to avoid any ambiguity among between different possible paths. Besides, precise synchronization is needed.

Another lightpath labeling scheme based on constant weight code label encoding [32],[33] has also been recently proposed. It was realized by embedding the label or low-speed data, which contained lightpath identification information, to the data signal by means of a complementary constant-weight code (CCWC). Electrical direct sequence code-division- multiple-access (CDMA) technique was employed to support simultaneous reception of multiple labels from different WDM signals, via single low-speed photo-detector. However, the CCWC would impose redundancy on the original data and violate the data speed and data format transparency. In addition, lightpath tracing or routing failure detection was performed at the intermediate network node and it

could only be applied to the optical network in which the routing path of each optical data packet has already been determined at ingress node. Similar techniques have been proposed to introduce lightpath labeling to the signals in differential phase shift-keying (DPSK) [34], dual polarization-differential quadrature phase shift-keying (DQPSK) [35] and optical orthogonal frequency division multiplexing (OFDM) [36] formats.

In this thesis, we propose a novel optical encoding scheme to realize path tracing in optical network. A distinct prime number was assigned as the path information tag for each network node. Through employing optical label encoders based on prime number multiplication at the outputs of the network nodes, path information tag was embedded to the optical packet label. All the path information tags carried by the optical data packet were easily extracted and identified by simple computation on the optical packet label at the receiving node. The all-optical label encoder can manipulate the label on-the-fly and support multi-wavelength's labels encoding operations simultaneously. In addition, it is a passive device which favors green photonics processing at the intermediate network nodes. Besides, any possible network looping problem in the optical network could also be identified.

2.2 Path Tracing Using Prime-Number Tags

In this section, we illustrate the principle of path tracing by employing the proposed prime number codes. There are two different approaches to realize path tracing, namely network node tracing and network link tracing. Network node tracing identifies all the network nodes that the optical data packet has traversed; while network link tracing identifies all the optical fiber links and the input/output ports of the network nodes that the optical data packet has traversed. Both of them can be realized using the proposed prime-number tags with slight modifications.

2.2.1 Network Node Tracing

Figure 2.1 shows an example of a wavelength routing network with six network nodes. Each network node comprises an AWG-based OXC and is assigned with a distinct prime number (starting from the value of 3), as the node identification tag. Each optical data packet comprises a data payload and a label. Its label starts with a value of 1 and will be multiplied by the tag values of all the individual network nodes that it has traversed along its whole path, via an optical encoder residing at each output port of the OXC. Note that the optical encoders on all output ports of the same OXC are identical, as they are performing the prime number multiplication with the same tag value. At the receiving node, the label of the received optical data packet is extracted and detected and its contained value is decoded for further prime-number factorization. The retrieved

prime-number factors imply the exact network nodes that the optical data packet has traversed.

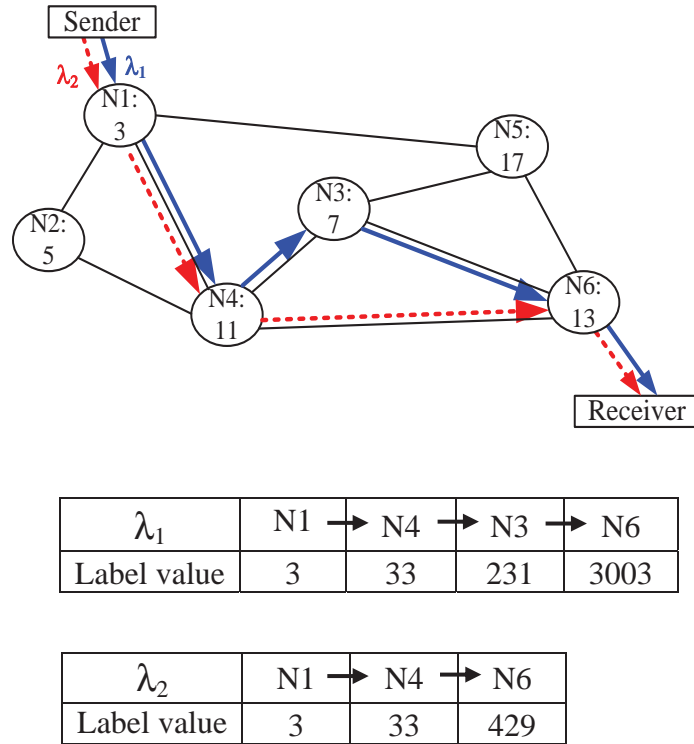


Figure 2.1 : An example wavelength routing network to illustrate the network node tracing scheme using the proposed prime-number tags. Node notation: N<node number>:<tag>.

Figure 2.1 illustrates two optical data packets on wavelengths λ_1 and λ_2 , as examples, and they travel from node N1 to node N6, via different paths. For the optical data packet carried on λ_1 , its label, with an initial value of 1, is multiplied by 3, 11, 7 and 13, as it traverses N1, N4, N3 and N6, respectively. The final label value at the output of N6 is 3003. As a result, the receiver can identify the traversed network nodes, by computing all prime-number factors in the received label value. For example, the identified traversed network nodes in Figure 2.1 are N1, N3, N4 and N6, according to the respective retrieved prime-number factors

(i.e. 3, 7, 11, 13) from the received label value of 3003. Similarly, the optical data packet carried on λ_2 traverses N1, N4 and N6, respectively, and the final label value at the output of N6 is 429. As a result, network node tracing is achieved.

2.2.2 Network Link Tracing

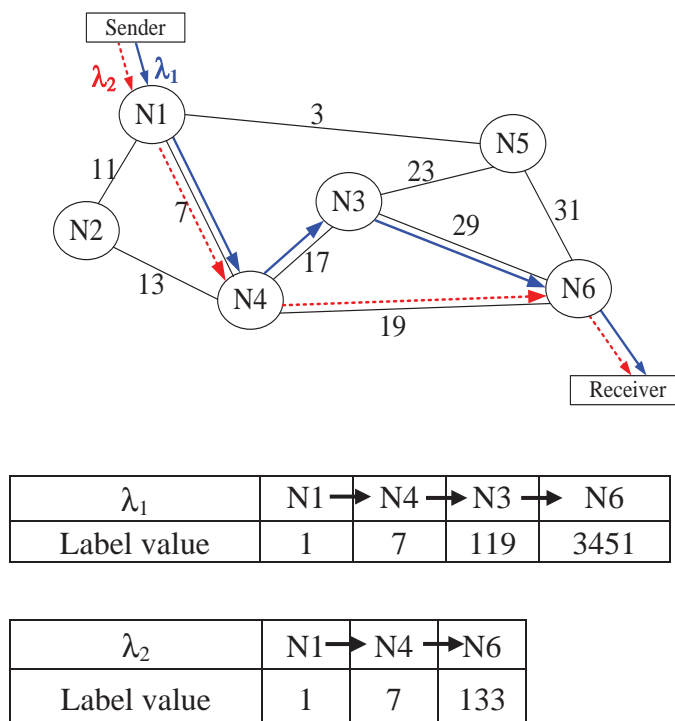


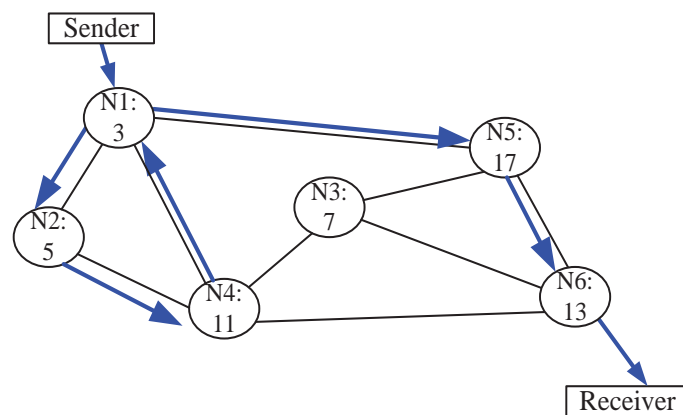
Figure 2.2 : An example wavelength routing network to illustrate the network link tracing scheme using the proposed prime-number tags. Each link is assigned a distinct tag value.

For the network link tracing, it can also be implemented using the prime-number tag identification as stated above with slight modification. Each fiber link of the optical network is now assigned with a distinct prime-number. Whenever the optical data packet passes through a particular fiber link, its label

will be multiplied by the prime-number tag assigned to that link. As a result, all the fiber links that the optical data packet has traversed can be identified at the receiving node, via prime-number factorization of the received label value. Figure 2.2 shows an example that the individual fiber links in the network have been assigned with their distinct prime-number tags.

Note that the chosen prime number values starts from 3 (instead of 2), to assure all of them are odd numbers. Thus, the least significant bit (LSB) of every prime number tag used is of value “1”, which is served as the start bit of the label, and also facilitates synchronization.

2.2.3 Network Looping Problem

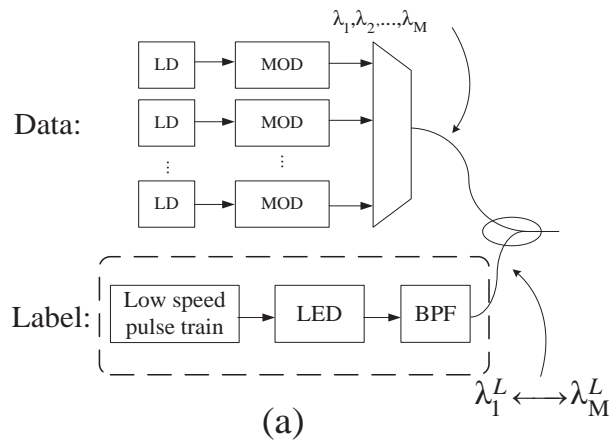


Node	N1	→	N2	→	N4	→	N1	→	N5	→	N6
Label value	3		15		165		495		8415		109395

Figure 2.3 : An example all-optical packet-switched network to illustrate network loop problem when using the network node tracing scheme. Node notation: N<node number>:<tag>.

Both the network node tracing and network link tracing are capable to detect any network looping problem. Whenever the same prime-number factor appears more than once in the result of prime-number factorization of the received label value at the receiving node, this indicates that the respective network node or network link has been traversed more than once and thus network looping may have occurred. Figure 2.3 illustrates an example of network node tracing when a network looping problem occurs. The optical data packet has traversed the network nodes in the sequence of N1, N2, N4, N1, N5, and N6. Thus, the label value retrieved at the receiving node (N6) is 109395, which can be factorized into the prime numbers of 3, 3, 5, 11, 13, and 17. Note that that the prime number 3 has occurred more than once. This implies the optical data packet has traversed network node N1 more than once. Hence, the network looping problem is identified.

2.3 Optical Implementation



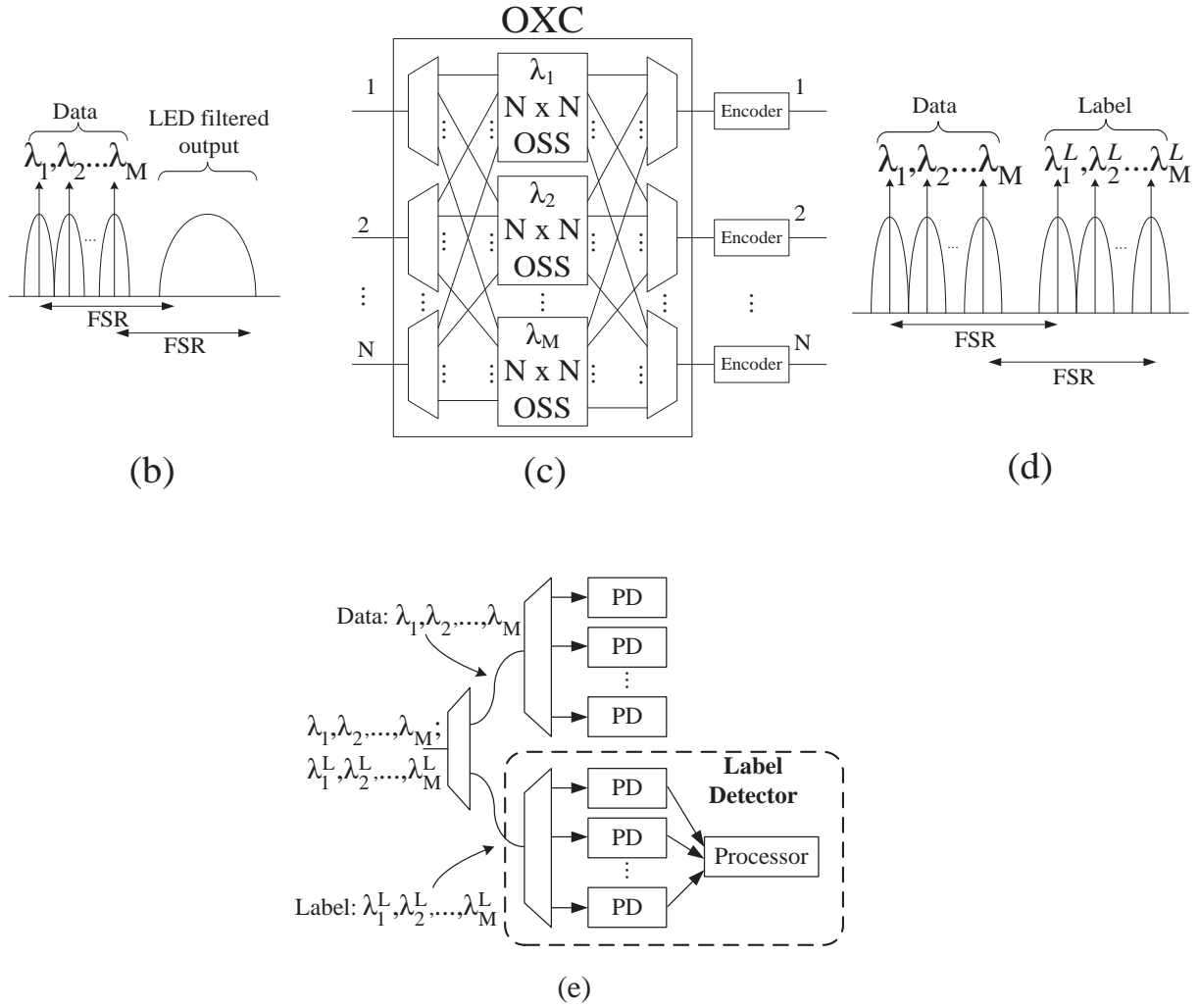


Figure 2.4 (a) Transmitter module at the ingress node. (b) Input signal spectra at ingress node input. (c) Structure of a network node with an encoder on each OXC output port for network node tracing. (d) Output signal spectra at output port of OXC. (e) Receiver module at the receiving node (PD: photodiode).

To realize path tracing in optical layer, a broadband light source, such as light-emitting-diode (LED), is employed, as one feasible realization approach. The structure of the transmitter is shown in Figure 2.4(a). LED's output is filtered with spectral range about one free-spectral range (FSR) of the AWG-

based OXC away from the data wavelengths ($\lambda_1, \dots, \lambda_M$), as shown in Figure 2.4(b), at the ingress node. All OXCs in the optical network are assumed to have the same FSR. The optical carriers for the labels ($\lambda_i^L = \lambda_i + \text{FSR}$; for $i=1, \dots, M$) of their respective data wavelengths are generated, via spectral slicing at the OXC, as in Figure 2.4(d). With the cyclic spectral property of the OXC, each label wavelength can pass through the same transmission passband of the OXC with its respective data wavelength.

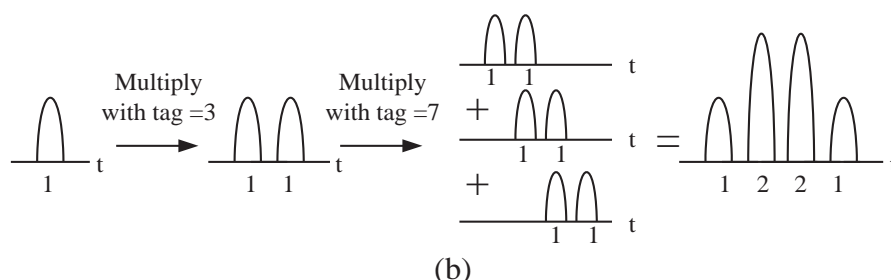
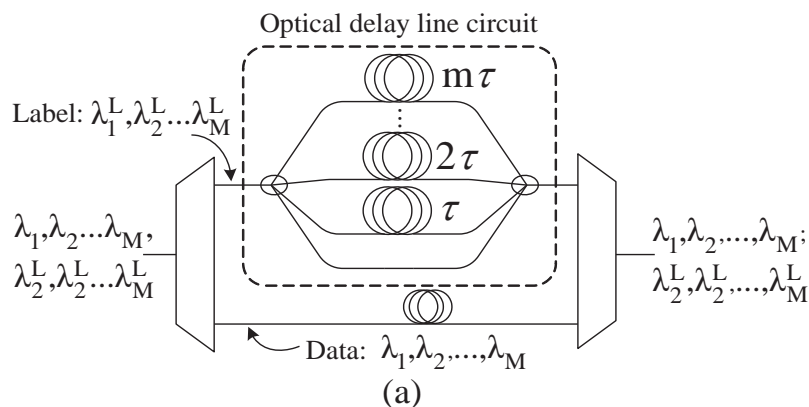


Figure 2.5: (a) Structure of the optical encoder for prime-number multiplication. (b) An example of multiplying original label valued “1” to tag “3” then tag “7”.

At the input of the ingress network node, the LED is modulated with a single optical pulse when the data wavelengths initiate to carry the optical data packets. Thus, each label wavelength starts with a single optical pulse (i.e. label

value=1). At each output port of the OXC, the switched data wavelengths and their corresponding encoded labels from different inputs are fed into an optical encoder to perform multiplication of its assigned prime-number tag to the incoming label, and its structure and principle are illustrated in Figure 2.5(a). The data wavelengths and the label wavelengths of the incoming composite signal are first separated such that the label wavelengths are fed into an optical delay line circuit for multiplication of the label values with the prime-number tag of the OXC. The optical delay line circuit comprises an optical power splitter, an array of fiber delay lines, followed by an optical power combiner. By setting appropriate number of fiber delay lines, it can generate an impulse response which represents a particular binary number. Thus the resultant output pulse sequence corresponds to the product of the input label value and the tag value.

For instance, as shown in the Figure 2.5(b), when an incoming label with a value of 1 (i.e. one optical pulses) is fed into the optical delay circuit with fiber delays of $0, \tau$, which represent a tag value of 3, the output will have two pulses with identical amplitudes and thus represent the decimal value of 3 in binary form. Next, the label further passes through another optical delay circuit with fiber delays of $0, \tau, 2\tau$, which represent a tag value of 7, the output will have four pulses with relative amplitudes 1, 2, 2, 1, respectively. By substituting these relative amplitudes as the coefficients of the polynomial expression, $1 \times y^3 + 2 \times y^2 + 2 \times y^1 + 1 \times y^0$ with $y=2$, a decimal value of 21 is obtained and this corresponds to the product of the input label value (3) and the tag value (7). Table 2.1 shows outputs of the optical encoder for different input label values.

Table 2.1: Examples of label multiplication at optical encoder

Input label value	Tag value (Impulse response)	Output label value
1,1= 3 (2-symbol)	1,0,1= 5 (3-symbol)	1,1,1,1= 15 (4-symbol)
1,1= 3 (2-symbol)	1,1,1= 7 (3-symbol)	1,2,2,1= 21 (4-symbol)
1,0,1= 5 (3-symbol)	1,1,1= 7 (3-symbol)	1,1,2,1,1= 35 (5-symbol)
1,1,1,1= 15 (4-symbol)	1,1,1= 7 (3-symbol)	1,2,3,3,2,1= 105 (6-symbol)
1,1,1,1= 15 (4-symbol)	1,0,1,1= 11 (4-symbol)	1,1,2,3,2,2,1= 165 (7-symbol)

At the label detector, the label wavelength of each received optical data packet is extracted and detected through the use of a low speed photodiode (PD), as shown in Figure 2.4(e). By examining the amplitudes of the detected label pulse sequences, the label value is determined. Through prime-number factorization of the label value, the traversed network nodes or network links by the received optical data packet can be derived, hence path tracing is achieved. Moreover, regarding to the performance of the label signal on each label wavelength, the accumulated noise and the accumulated fiber chromatic dispersion, are far less stringent than that of the high-speed data packet. With proper design of signal transmission on the fiber-optic links, the quality of the optical data packet, as well as the label signal can be assured. On the other hand, although LED is used as the light source for the label signals, spontaneous-spontaneous beat noise from the LED as well as chromatic dispersion during fiber transmission tolerance can be substantially relieved by employing low-bandwidth receiver and the spectral slicing inside the OXCs [48]. The signal-to-

noise ratio due to optical beating is proportional to the ratio of the optical bandwidth to the electrical bandwidth. Therefore, by using a low-bandwidth receiver, the signal-to-noise ratio can be enhanced.

From the structure of the label encoder, it manipulates the label on-the-fly all-optically and also supports multi-wavelength label encoding operations, simultaneously. Standard single mode fibers (SMF) can be used as the delay elements in the proposed optical label encoder. Due to the intrinsic chromatic dispersion in the fiber, the group delays experienced by different wavelengths may have minor differences. Nevertheless, as long as the minimum unit of delay in each wavelength is larger than the pulse width of the label bits, the pulses will not overlap with each other and thus the pulses can still be properly detected. For instance, in our investigation, 1.5-meters fiber is used to introduce 1-bit delay. The group delay difference induced by chromatic dispersion effect is very small, due to the short length of fiber. With the relatively low data rate of the label pulses (say 150 MHz, for example), the possible inter-symbol interference (ISI) effect caused by chromatic dispersion in such short length of fiber is insignificant. Also, any possible length variation (say < 10 cm) in the fiber delay lines in the proposed optical encoder would not induce excessive misalignment of the optical pulses on different delay arms within the same time slot during the pulse power addition process.

Besides, the proposed optical encoder is a passive device which favors green photonics processing at the intermediate network node. It can also be implemented with planar-lightwave-circuit (PLC) [49] which is compact and

integrable. Moreover, with the current device fabrication technology, the uniformity of the insertion losses of all output ports of the $1 \times M$ optical splitter in the optical encoder can be less than 2 dB when M is 64 [50]. With the nature of simple addition of the pulse power in the same respective delayed time-slot, the differences in various amplitude levels in the detected label signal should be large enough to differentiate among themselves, as both data and label wavelengths are amplified by EDFAs across the network. Thus, the influence to the identification of the prime number tag carried in the label is very minimal.

In addition, the detection of the label value requires electronic signal processing procedures to identify different amplitude levels of various detected pulses. This could be easily implemented using conventional digital signal processing (DSP) modules. There may be time misalignment between the first bit of the optical data packet and the label due to chromatic dispersion. However, precise synchronization or dispersion management are not needed. As all the encoded label values are in odd numbers, due to the prime number multiplications, there is always a bit 1 present at the first bit (least significant bit) of the label. Therefore, we can always regard the first detected pulse as first bit of the label. However, there should be enough guard time before or after the packet to ensure that each packet label should not exceed the packet length. On the other hand, the peak powers of the label pulses should be controlled to ensure that they are always transmitted in linear transmission regime. To avoid the generation of label signal with too-high peak pulse power during prime number tag multiplication process at the optical encoder, we may employ a larger prime

number set and may assign only those prime numbers which have fewer number of 1-bit in their binary forms, at the expenses of longer fiber delay required.

In the proposed path tracing scheme, distinct prime-number tags are assigned to all networks nodes or links, so as to facilitate the path tracing via prime-number tag multiplication at the intermediate nodes and prime-number factorization at the receiving node. Optical encoders of the same tag values are placed at all output ports of the OXC, for network node tracing, while that of distinct tag values are placed at individual output ports of the OXC to label the connected outgoing fiber links, for network link tracing. The operator should keep an inventory record of all the prime-number tags employed in the network, and the tag assignment for existing network resources is usually kept unchanged. Any newly added network node or link should be assigned with a new and distinct prime-number tag so as to uniquely identify the new network resource. The path tracing scheme primarily aims to retrieve the traversed physical path of the data packet, and compare with information at the control plane so as to detect the possible routing error.

2.4 Experimental Results

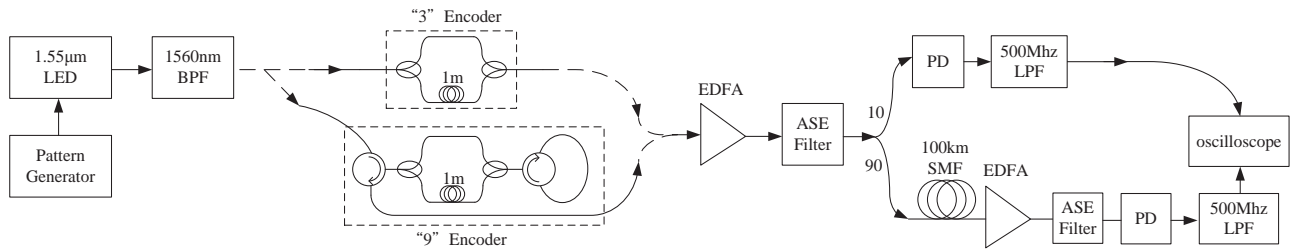


Figure 2.6: Experimental setup for the “3” encoder and “9” encoder.

The feasibility of the optical label encoder has been demonstrated by a proof-of-concept experiment. Figure 2.6 shows the experimental setup. A 1550-nm LED having 30-nm bandwidth was directly modulated with a 20-MHz electrical pulse train signal. After passing through an optical filter with a center wavelength of 1560 nm and a transmission passband of 0.8 nm, it was then fed into an optical encoder to multiply a decimal value of 3 or 9 (denoted respectively as a “3”-encoder or “9”-encoder). The “3”-encoder comprised two separate fiber branches, each had 0 and 4.45-ns relative fiber delays, respectively, sandwiched by a pair of 1 × 2 optical splitters/combiners (as label bit rate was ~225 Mb/s). The “9”-encoder was simulated by transmitting the “3”-encoder twice via an optical circulator, as depicted in Figure 2.6.

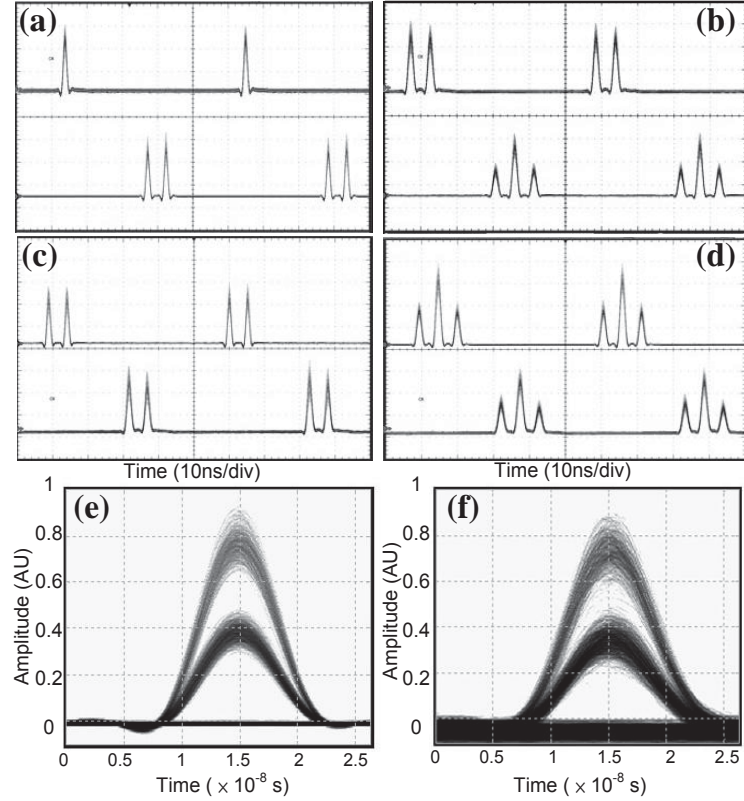


Figure 2.7: “3” optical label encoder outputs (lower trace) with inputs (upper trace): (a) “1”, (b) “1,1”. Waveforms after 100-km transmission (lower trace) with encoded outputs (upper trace) (c) “1,1”, (d) “1,2,1”. The eye diagram of encoded pattern “1,2,1” (e) before transmission and (f) after transmission.

Considering the case of the “3”-encoder, the obtained optical encoder outputs were shown in Figure 2.7(a)-(b), when the inputs are “1” and “1,1” (i.e. decimal values: 1, 3), respectively. Their respective relative pulse amplitudes were “1,1” and “1,2,1”, which correspond to decimal values of 3 and 9 respectively. Figure 2.7(c)-(d) show the optical encoder outputs after 100-km SMF transmission. Figure 2.7(e)-(f) show the eye diagrams of encoder output “1,2,1” before and after fiber transmission, respectively. Similarly, Figure 2.8(a)-(b) show the optical encoder outputs of the “9”-encoder with the inputs “1” and

“1,1” respectively. Their respective relative pulse amplitudes were “1,2,1” and “1,3,3,1”, which correspond to decimal values of 9 and 27 respectively. The waveforms before and after fiber transmission have been shown in Figure 2.8(c)-(d) with the eye diagrams shown in Figure 2.8(e)-(f).

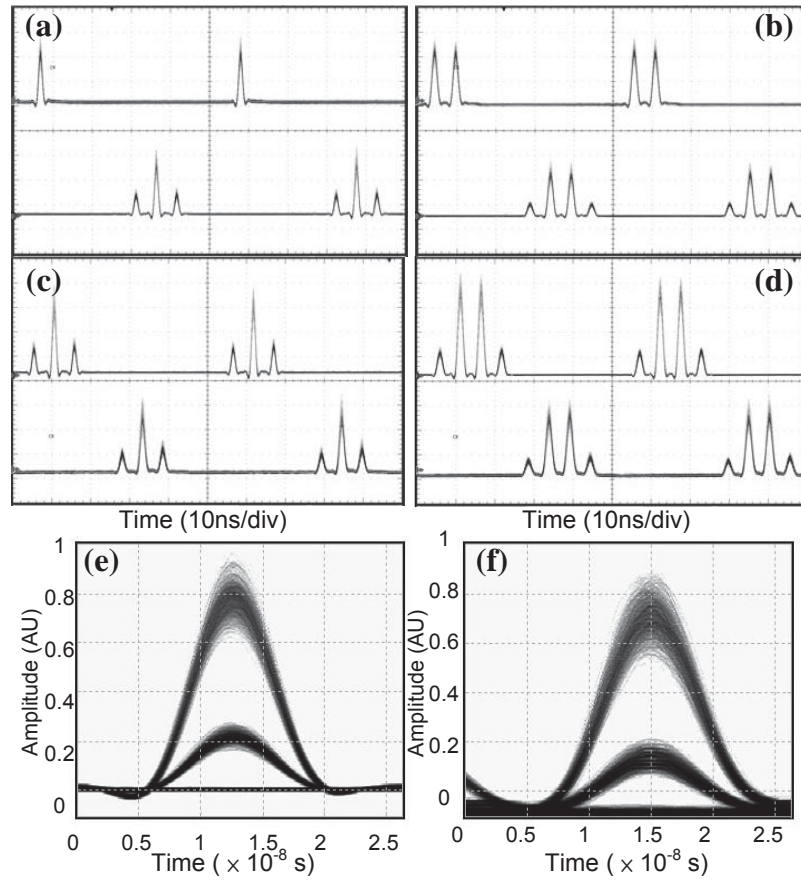


Figure 2.8 : “9” optical label encoder outputs (lower trace) with inputs (upper trace): (a) “1”, (b) “1,1”. Waveforms after 100-km transmission (lower trace) with encoded outputs (upper trace) (c) “1,2,1”, (d) “1,3,3,1”. The eye diagram of encoded pattern “1,3,3,1” (e) before transmission and (f) after transmission.

The detection of the pulse amplitudes was performed by electronic processing with properly-set threshold levels. The signal quality could be further

enhanced by performing electronic digital filtering and equalization techniques. Figure 2.9 shows the eye diagrams of the detected label signal waveforms after further being fed into a 3-tap feed forward equalizer (FFE). Much clearer eyes were observed, as compared with those depicted in Figure 2.8 (e) & (f), respectively. In general, the above measurements have proved the integrity of the proposed optical encoder for prime number multiplication.

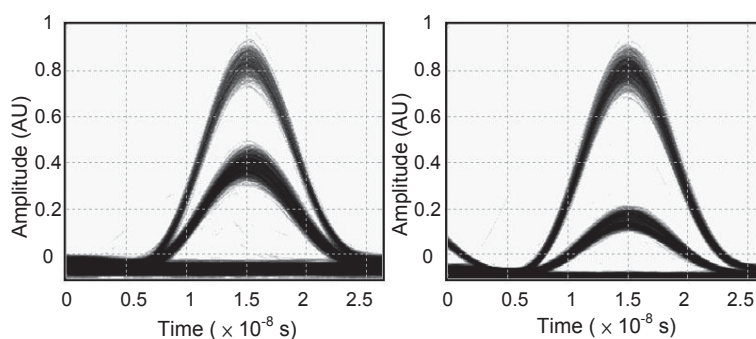


Figure 2.9 : The eye diagram of equalized waveform after 100-km SMF transmission with pattern: (a) “1,2,1”, (b) “1,3,3,1”.

2.5 Multi-Level Amplitudes Of The Label

When an optical packet traverses across the network, its label value is multiplied, via the encoders, along its path. As the hop count increases, the label value is getting larger and the pulses contained in the label signal would exhibit multiple amplitude levels. We have investigated the issues of peak-to-average power ratio (PAPR), as well as the required number of resolution bits for the analog-to-digital converters (ADCs) required for proper retrieval of the label signal value.

Basically, PAPR is a common measure for the orthogonal frequency division multiplexed (OFDM) communication systems [51]. It should be kept at low values, as the signal with high PAPR value would be very susceptible to nonlinearities in fiber and other in-line optical components. Figure 2.10(a) and (b) show the cumulative distribution (CDF) of the PAPR values of 10000 simulated final label signals with multi-level pulses under the case of different network sizes, ranging from 10 to 50 and has traversed over six nodes (hop count = 6) along its paths, as well as the case of different number of hop counts in a 50-node network, respectively. It was shown that most cases fell into the PAPR range from ~3 dB to ~4.5 dB. Such relatively low PAPR values enabled linear transmission of the label signals. Any increase in network size or hop count would only tend to increase the PAPR values slightly.

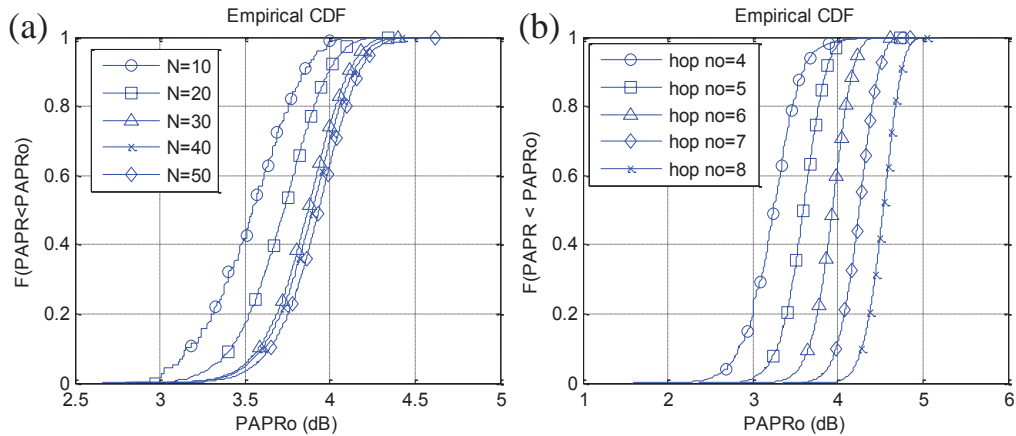


Figure 2.10 : Cumulative distribution of PAPR of the encoded label waveforms (a) different network size with hop no = 6. (b) Different hop no with 50 network nodes.

On the other hand, the increase in the number of amplitude levels of the label signal, due to large label values, would require much larger resolution of the

electronic ADC chips to differentiate and recognize the individual amplitude levels. Figure 2.11 (a) shows the required number of the ADC under different network sizes and hop counts. 10000 label values were simulated. The results showed that the required number of ADC resolution bits was much less sensitive to the increase in network size, but increased linearly with the increase in hop count. It could be further reduced by employing a larger prime number set and selecting those which contained fewer number of 1-bit in their binary form. Figure 2.11 (b) shows the reduced ADC resolution required for networks having the prime number tags with less than or equal to four bit-1.

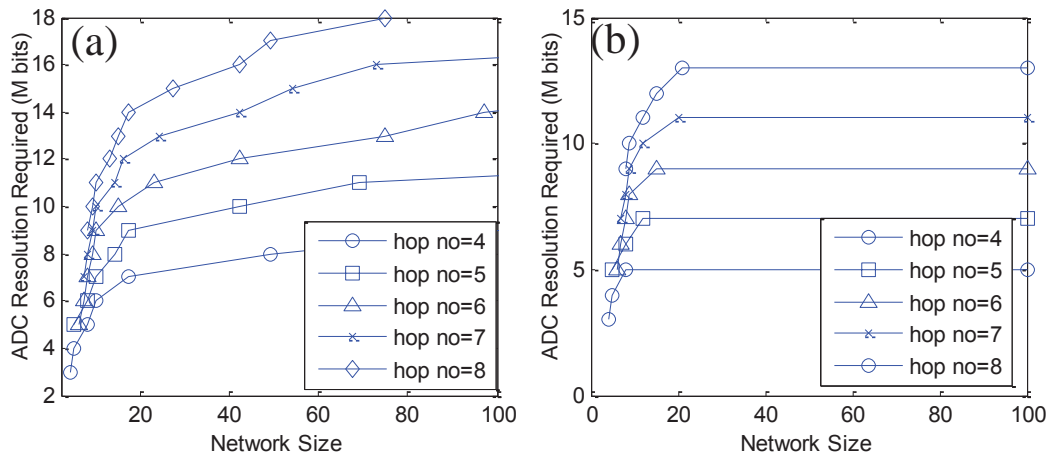


Figure 2.11 : The ADC resolution required with different network sizes. (a) without prime number selection, (b) with prime number selection. (Note the difference in Y-axis scale for both graphs)

2.6 Required Maximum Fiber Delay

In [23]-[26], several schemes based on different time-delay recognition were proposed to identify the state of input-output connections in OXCs. Basically, they could also be applied to realize path tracing with some modifications. Under network node tracing, the different time-delay recognition scheme in [23],[24], requires 2^{i-1} fiber delays at the i^{th} OXC. Therefore, given a maximum fiber delay D , it can support up to $\lceil \log_2(D)+1 \rceil$ OXCs in the optical network. The K -split multi-delay scheme in [25],[26] would not provide much improvements, as it is only advantageous when the number of ports in each OXC is large. On the other hand, our proposed scheme performs multiplication of prime numbers. It is well known that the total number of prime numbers less than a positive number Y , can be approximated by $\lfloor Y/(\ln Y) \rfloor$. The largest prime number less than Y can be represented in binary form with the number of bits less than or equal to $\log_2(Y)$. Therefore, given a maximum fiber delay D , it is a reasonable approximation that the proposed scheme can support up to $2^D/\lceil \ln(2^D) \rceil$ OXCs in an optical network. Fig. 13 shows the comparison of the required maximum fiber delay between the different time-delay recognition schemes [23],[24] and our proposed scheme, under network node tracing. It shows that our proposed scheme is much less sensitive to the network size.

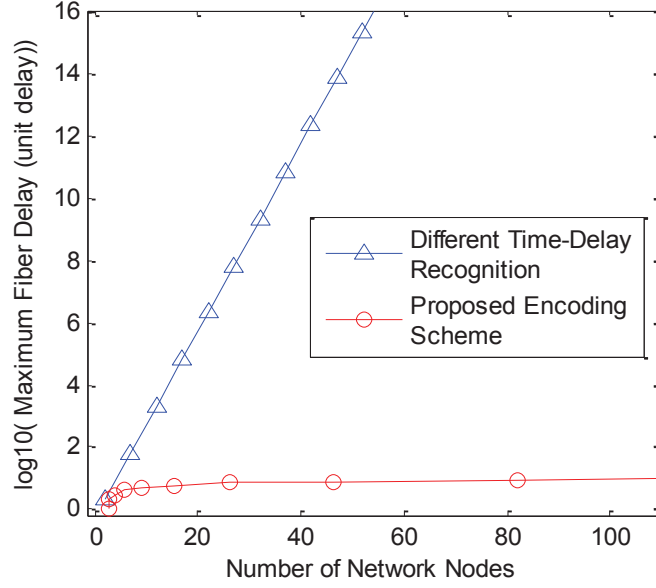


Figure 2.12: Maximum fiber delay required for different time-delay recognition scheme [23],[24] and our proposed encoding scheme under different number of OXCs in the optical network for network node tracing.

Considering network link tracing with L ports per OXC at each network node, each OXC port has a distinct identifier. Thus, the number of distinct identifiers required will be L times larger than that in the network node tracing case. Hence, our proposed scheme can support up to $2^D/[L\ln(2^D)]$ OXCs in an optical network. Considering the different time-delay recognition [23],[24] and K -split multi-delay scheme [25],[26], when the number of OXCs is N and each OXC contains L ports, the maximum fiber delays required are $[L(L+1)^{N-1}]$ and $[L\lceil \log_2(L+1) \rceil^{N-1}]$, respectively. Fig. 14 shows the scalability comparison among the different time-delay recognition scheme [23],[24], K -split multi-delay scheme [25],[26], the bit-pattern encoding and our proposed scheme. It is shown that that our proposed scheme requires far less maximum fiber delay than those previously described ones, under network link tracing. Table 2 summarizes the

comparison of different path tracing schemes, in terms of the length of the maximum fiber delay required.

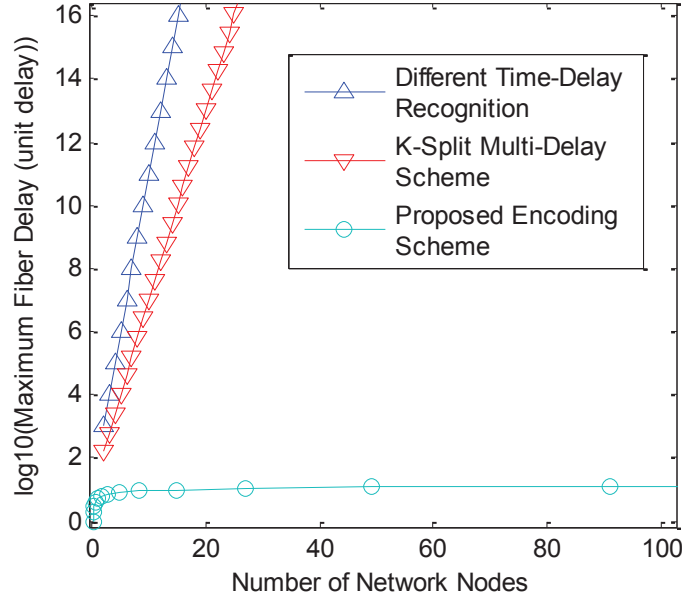


Figure 2.13: Maximum fiber delay required for time-delay recognition schemes and our proposed encoding scheme under different number of OXCs in the optical network for network link tracing.

Table 2.2: Comparison of required maximum fiber delay under different path tracing schemes. (D : maximum fiber delay, N : number of nodes, L : number of ports at each node)

	Maximum Fiber Delay, D		
	Different Time-Delay Recognition [23],[24]	K-Split Multi-Delay Scheme [25],[26]	Proposed Encoding Scheme
Node Tracing	$D=2^{N-1}$	N/A	$N=2^D/[\ln(2^D)]$
Link Tracing	$D=L(L+1)^{N-1}$	$D=L\lceil \log_2(L+1) \rceil^N - 1$	$N=2^D/[L\ln(2^D)]$

We should also notice that the maximum splitting ratio of the splitter used by the encoders is closely related to the maximum fiber delay D . More concisely

speaking, the maximum fiber delay D is the upper bound of the maximum splitting ratio of the splitters. As the splitting ratio of the splitter affects the amplitude reduction of the label pulses, the splitting ratio of the splitters should be minimized when the network size increases. In the above discussion, we notice the maximum fiber delay D has good scalability when the network size increases. Besides, the label pulses can easily be amplified simultaneously with the data channels using the EDFAs located at the output ports of the OXCs.

2.7 Summary

In this chapter, we have proposed the use of prime-number tag as a distinct identifier to label each network node or network link so as to realize path tracing in an optical packet-switched network. Possible network looping problems can also be identified. Prime-number multiplication can be performed using our proposed optical label encoder employing a specialized optical delay line circuit. The proposed optical label encoder is an all-optical and passive device, and supports simultaneous multi-wavelength and bi-directional operations. The proposed path tracing scheme can greatly facilitate the network management of an all-optical packet-switched network.

Chapter 3 A Novel Fiber-based Variable All-Optical Packet Buffer based on Self-Phase Modulation Induced Spectral Broadening

In this chapter, we propose a novel optical delay control mechanism to realize variable all-optical packet buffering, in which the amount of optical delay is controlled by the input signal power level. It consists of a passive fiber delay loop followed by an optical power dependent filter, which is realized by means of two stages of self-phase-modulation induced spectral broadening and offset-filtering. The feasibility of the proposed optical packet buffer has been investigated through numerical simulations and experiments. No polarization control and additional laser source is needed.

3.1 Introduction

In future optical packet switching (OPS) systems, data buffering is essential to resolve possible packet contention and it is considered as one of the greatest challenges in optical implementation. Although electronic buffer technology has been greatly improved recently, optical buffering is still an ideal candidate for future ultrahigh-speed transparent optical networks, as it does not require optical-electrical-optical (O-E-O) conversion and supports ultrafast data rates. In addition to data rate transparency, the absence of O-E-O conversion leads to much better power saving and reduced implementation cost. There are different categories of optical delay lines, including continuously tunable ones or

discretely variable ones. They have found applications in optical coherence tomography, optical control of phased array antennas for radio frequency communication, bit-level synchronization for interleaving, demultiplexing and switching, tapped delay lines for equalization, filtering, and chromatic dispersion compensation, etc. Nevertheless, the possible data packet buffering required for contention resolution in OPS systems might require relatively long fiber or expensive wavelength converter with large tunable wavelength range, when it was implemented by wavelength conversion followed by dispersive medium with group velocity dispersion [3],[4]. One interesting example is to convert the wavelength of the incoming data packet before being fed into a wavelength dependent delay element, where the signals at different wavelengths would experience different amount of temporal delays [8]. Another kind of optical delay lines was based on slow light induced by stimulated Brillouin scattering (SBS) [9],[10]. Nevertheless, their applications might be limited by the small amount of induced delay and the possible severe signal degradation at increased delay values.

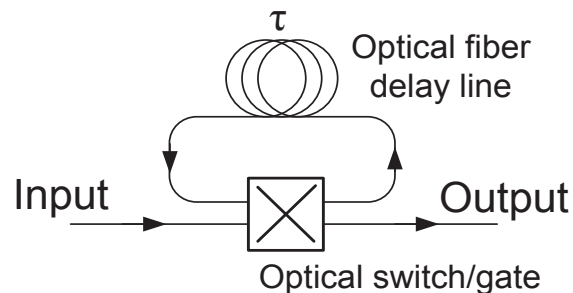


Figure 3.14 : The structure of re-circulating delay loop.

Figure 3.14 shows a common way to implement optical buffers based on an optical re-circulating loop, which required all-optical switches [13], optical switching via semiconductor optical amplifiers (SOAs) [14],[15] or through nonlinear polarization rotation inside the SOA [16], to control the number of circulations for the optical packet. However, it required synchronization between the switching time and the cycle of the packet propagation. In [17], an optical re-circulating loop with an optical thresholding function was used to control the propagation of low priority signal inside the loop, via wavelength conversion, so as to resolve the contention. In [18], the signal's wavelength was shifted by a certain amount after each cycle of circulation in an optical re-circulating loop, thus the output wavelength could be varied and controlled. In this paper, we propose an all-fiber variable optical packet buffer, in which the amount of delay is controlled by the input signal power level. The delay control is based on self-cloning the input optical signal, followed by optical power dependent filtering. The suggested optical sub-system implementation comprises a passive optical delay loop circuit and two stages of self-phase modulation (SPM) in highly nonlinear fiber (HNLF), followed by offset filtering. Due to the intrinsic nature of SPM, it does not require polarization control and no additional laser source is required.

3.2 *Input signal power dependent delay*

Having considered the pros and cons of the previously reported schemes for the implementations of variable optical buffer, we propose a novel all-fiber variable optical packet buffer architecture, which is based on a passive optical delay loop to provide long and discretely variable optical delay. The amount of optical delay induced is varied by controlling the input signal power level. Hence, simple optical data packet buffering in an optical packet switching system can be realized.

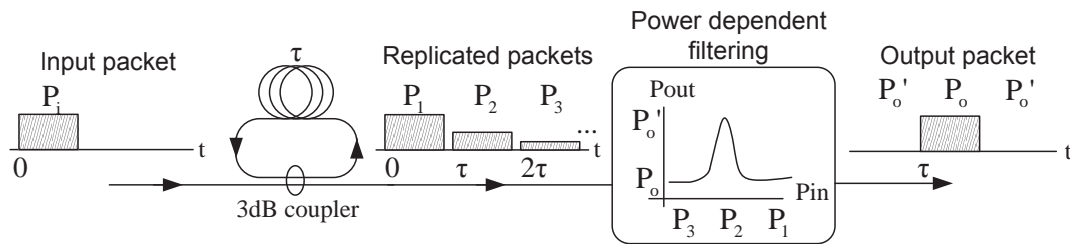


Figure 3.15 : Illustration on the delay control mechanism of the proposed optical packet buffer structure.

Figure 3.15 illustrates the principle of the delay control technique for the proposed optical packet buffer. The incoming optical packet with power P_i , first passes through a passive optical delay loop circuit to generate copies of the packets, temporally spaced by a fixed time interval, τ . The power of each delayed packet copy is designed to be 3-dB lower than its previous one, and this is to create a mapping between different time delays and different input signal power

levels. Therefore, optical packets having powers at P_1, P_2, P_3, \dots , will appear at time instances of $0, \tau, 2\tau, \dots$, respectively, as illustrated in Figure 3.15. As a 3-dB power coupler is employed, $P_2 = P_1/2, P_3 = P_1/4$, and so on. The generated optical packet train then undergoes optical power dependent filtering operation. As a result, only the optical packet copy at the specified power level (e.g. P_2) with the desired respective time delay (e.g. τ), remains at the output, while other packet copies are dropped or suppressed. The optical power dependent filter should be designed to have good power contrast between the transmission peak and floor, that is $P_o \gg P_o'$, as in Figure 3.15, so as to achieve good extinction ratio in the output signal. Hence, such optical subsystem transforms different input signal power level into different amount of time delay. The control of the time delay is achieved by altering the input signal power P_i such that the packet copy with the desired time delay and optical power level falls into the passband of the optical power dependent filter. Increasing the input signal power by 3 dB effectively induces an additional delay of τ . Ideally, the optical power of the output packet should be the same while the amount of delay varies.

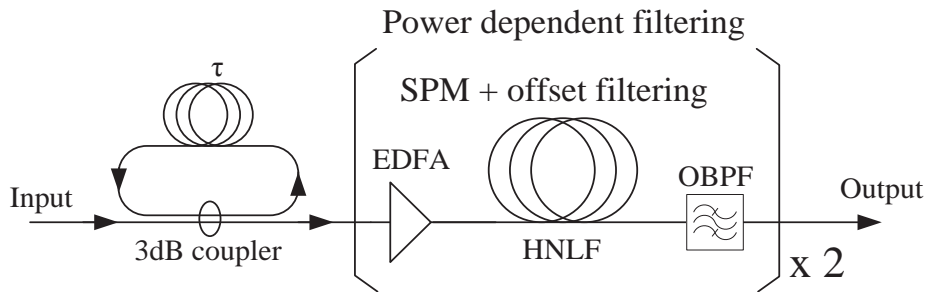


Figure 3.16 : An optical implementation of the proposed optical buffer.

Figure 3.16 depicts a feasible implementation of the proposed optical packet buffer. It comprises a passive optical delay loop circuit, as described before, and an optical power dependent filter, where two stages of SPM in HNLF, with offset-filtering are employed. The technique of employing SPM in HNLF with offset-filtering has been widely studied in optical 2R signal regeneration [52]-[55] and was recognized as Mamyshev regenerator. It offers simple structure to perform noise suppression at zero level, in addition to amplitude equalization.

The input optical data packets are assumed to be modulated in return-to-zero pulsed format. In the first stage of SPM and offset filtering, spectral broadening of the optical pulses induced by SPM in HNLF creates multiple lobes in the spectrum [56], where the outermost lobes, located farther away from the center wavelength, contribute to higher signal power. In addition, the width of the broadened spectrum is increased with the input signal power. Any further increase in input signal power would lead to supercontinuum generation, where the output signal power is dispersed across a wide wavelength range. By optimal setting of the optical bandpass filter (OBPF) so as to filter out the outermost spectral lobes of the signal at the specified input signal power, only the optical packet copy with pulses at the same specified power level and the respective desired time delay, remains at the output; while other packet copies are dropped or suppressed. Thus, input signal power dependent filtering operation is realized. The second stage of SPM and offset-filtering performs optical power

thresholding function so as to further enhance the extinction ratio between the output packet and the dropped packet copies.

3.3 Numerical Simulation Studies

In this section, the feasibility of this scheme has been investigated and characterized through numerical simulations. The simulation setup is shown in Figure 3.17. The output from a 10-GHz mode locked laser with 2.5-ps pulse width at 1547.38 nm was first modulated by an optical intensity modulator, generating an input optical packet with 20-bit pulse pattern. Then it was fed into a passive optical power splitter connected with different fiber delay lines and attenuation values in order to simulate the output of the passive delay loop circuit, in form of multiple copies of the input signal. Each subsequent delayed copy experienced an additional time delay of 3.5 ns and its power was relatively reduced by 3 dB, accordingly. The generated packet train then passed through two stages of SPM in HNLF and offset filtering to perform optical power dependent filtering and power thresholding operations. In the first stage, a piece of 1-km dispersion-flattened highly nonlinear fiber (DF-HNLF) was used as the nonlinear medium and its nonlinear coefficient, zero-dispersion wavelength and dispersion slope were $10.8 \text{ W}^{-1}\cdot\text{km}^{-1}$, 1550 nm and $0.007 \text{ ps}/(\text{nm}^2\cdot\text{km})$, respectively. The spectrally broadened signal was then filtered at 1541 nm, via a 0.8-nm bandwidth OBPF to realize power dependent filtering. After being amplified via an Erbium-doped fiber amplifier (EDFA), the output signal was then fed into the second stage of SPM and offset filtering to perform power

thresholding. In this stage, a piece of 2-km dispersion-shifted highly nonlinear fiber (DSF-HNLF) was employed and its nonlinear coefficient, zero dispersion wavelength and dispersion slope were $11.9 \text{ W}^{-1}\cdot\text{km}^{-1}$, 1544nm and $0.018 \text{ ps}/(\text{nm}^2\cdot\text{km})$, respectively. The output signal is then filtered by another 0.8-nm OBPF at the wavelength 1535.5 nm .

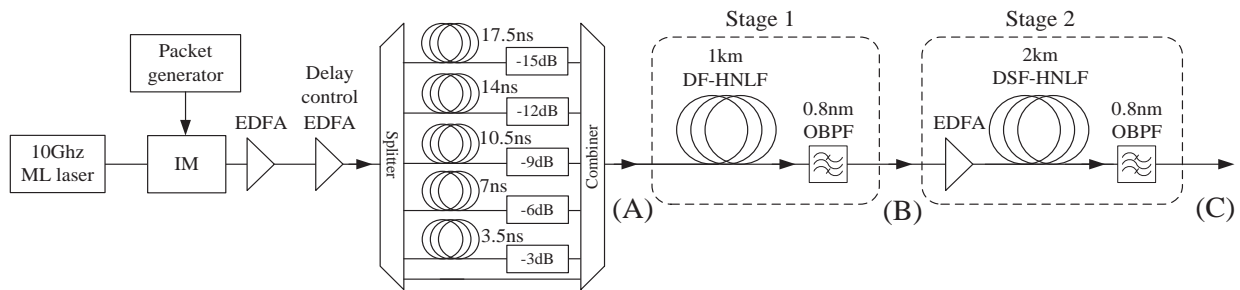


Figure 3.17 : The simulation setup. (ML laser: mode-locked laser, IM: intensity modulator, OBPF: optical band pass filter)

First, the power transfer characteristics of the proposed optical packet buffer were studied using an unmodulated optical pulse train, as the input signal. Figure 18 shows the output power of the two stages of SPM followed by offset filtering when optical pulses at different power levels were inputted to the proposed optical packet buffer. The power filtering effect was observed at the Stage 1 output (measured at point B in Figure 3.17), which exhibited a maximum output when the input signal power was at about 15 dBm, while power thresholding operation was observed at the Stage 2 output (measured at point C in Figure 3.17), which further enhanced the power contrast between the peak output power and its adjacent power trough in the power transfer curve. Figure

19 shows the optical spectra measured at the output of Stage 1 at different input signal power levels, where the input power level were subsequently increased by 3 dB, so as to realize the same condition as in the multiple delayed copies at the output of the passive optical delay loop circuit. The insets in Figure 19 show the enlarged diagram of the respective optical spectra. At low input signal power, more power was observed to be concentrated at the outer spectral sidelobes, while at high input signal power, supercontinuum generation occurred. The position of the offset filter at Stage 1 output was marked as the dotted line (at 1541 nm) in Figure 19. When the input pulse train was at the optimum power, say 14.88 dBm, for example, one of the outer spectral sidelobes fell into the passband of the offset filter and thus its filter output gave a maximum power level. The other input pulse trains having lower input power levels did not get sufficient spectral broadening from SPM, thus their filter outputs were at very low power level.

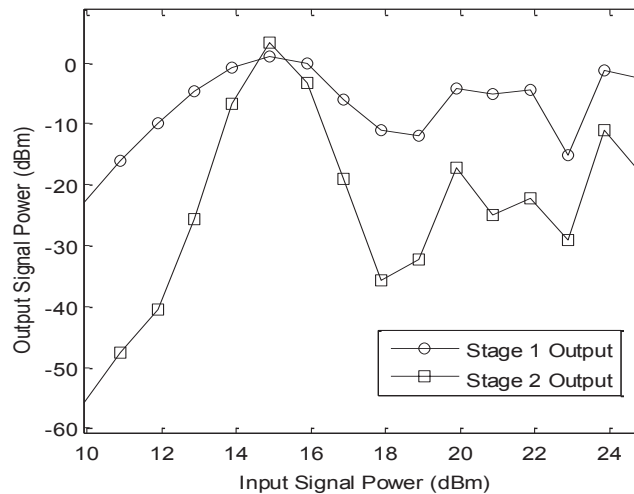


Figure 18 : The simulated power transfer curves of Stage 1 output and Stage 2 output of the proposed optical packet buffer.

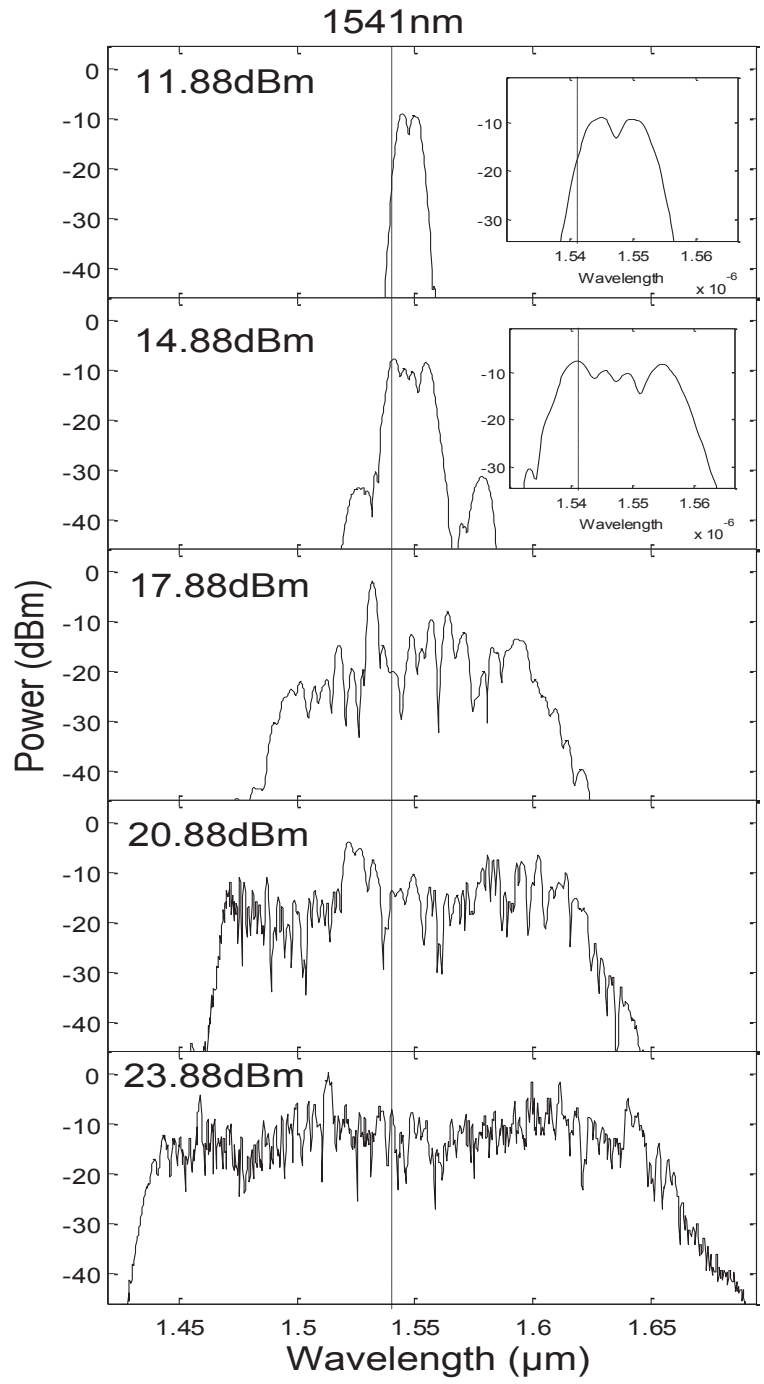


Figure 19 : The simulated optical spectra of the input pulse train at the output of Stage 1 with different input signal power levels into the HNLF.

On the other hand, the input pulse train with power higher than the optimum level would give low power at the filter output, since the excess power had led to subsequent spectral broadening induced by the mixed effects of SPM, four-wave-mixing (FWM) and Stimulated Raman Scattering (SRS), and thus resulted in supercontinuum generation. Hence, the power of the input signal would get dispersed across a wide wavelength range and led to lower power level at filter output.

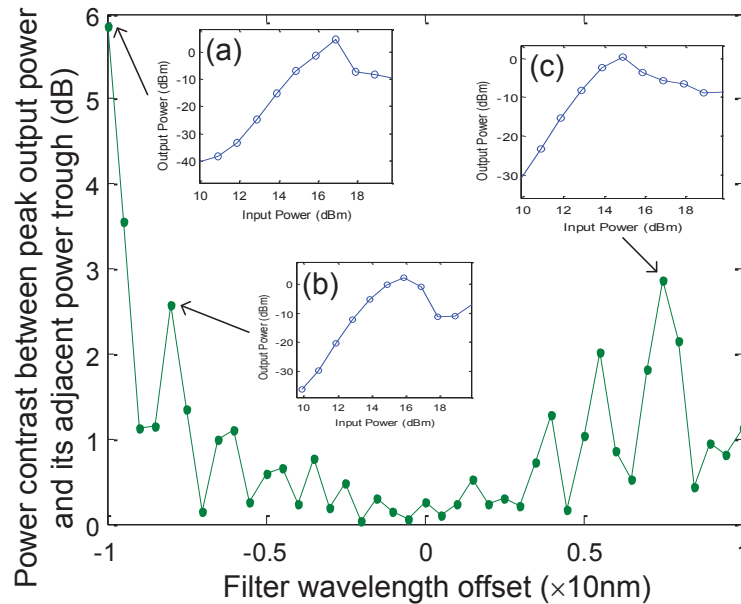


Figure 20 : Simulated power contrast between the peak output power and its adjacent power trough of Stage 1 outputs with different filter wavelength offset values with respect to the input signal wavelength. The insets show the power transfer curves when the filter wavelength offsets were set at (a) -10nm, (b) -8nm, (c) +7.5nm, respectively.

Figure 20 shows the simulated power contrast between the peak output power and its adjacent power trough at Stage 1 output when the filter wavelength offset was varied from +10 nm to -10 nm, with respect to the input signal wavelength. The insets in Figure 20 further show the power transfer curves at

different filter wavelength offset values at (a) -10 nm, (b) -8 nm, and (c) 7.5nm. The results show that such power contrast in the power transfer curve at Stage 1 output increased with the filter wavelength offset value. Although higher power contrast in the power transfer curve was more desirable for more effective power dependent filtering, the respective input signal power required to achieve the respective peak output power was found to be increasing with the filter wavelength offset value, as illustrated in Figure 21. Hence, there existed a tradeoff between the power contrast and the required input signal power in the power transfer curve at Stage 1 output.

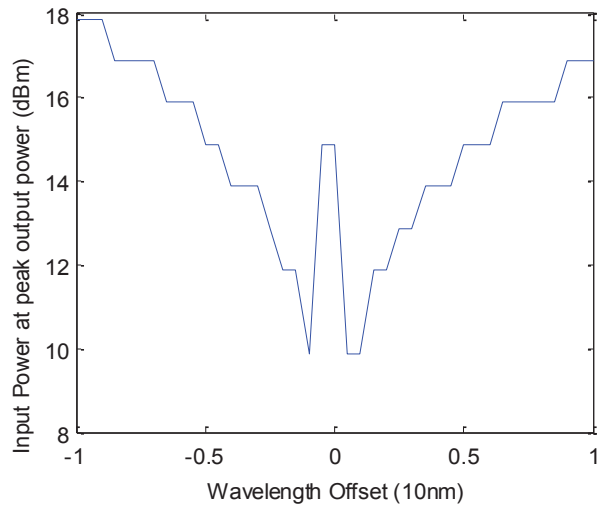


Figure 21 : Required input signal power of Stage 1 at peak output power with different filter wavelength offset values.

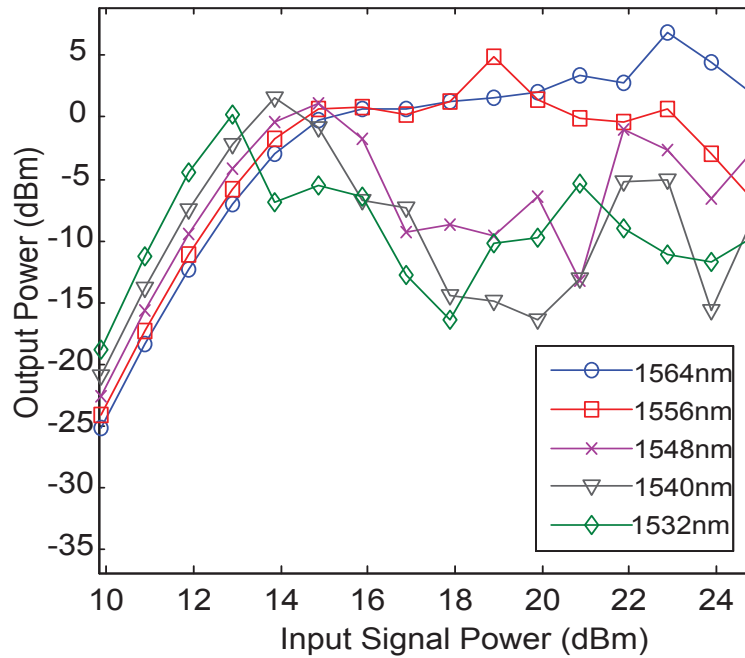


Figure 22 : Simulated power transfer curves at Stage 1 output for HNLFs with different HNLF zero-dispersion wavelengths, given the input signal wavelength is 1547nm.

Besides, the effect of the zero-dispersion wavelength of the HNLF employed in Stage 1 also imposed significant impact to the performance of the power dependent filtering operation. Figure 22 depicts the power transfer curve at Stage 1 output when the zero-dispersion wavelength of the HNLF employed was varied from 1532 nm to 1564 nm, given that the input signal wavelength was chosen at 1547 nm. It is shown that when the input signal wavelength was set in the anomalous dispersion regime (HNLF zero-dispersion wavelengths at 1532nm, 1540nm), the power filtering effect was quite prominent with good power contrast within a narrow input power range in the power transfer curve. This could be attributed to the fact that the signal peak power would reach a higher level, due to the pulse compression effect in the anomalous dispersion regime,

thus could help to foster the power dependent filtering with better power contrast. However, due to the possible coherence degradation of the output signal when being operated in the anomalous dispersion regime [57]-[59], we had better operate the input signal in the normal dispersion regime, which corresponded to the power transfer curves with their respective HNLF zero-dispersion wavelengths at 1548nm, 1556nm, and 1564nm, in Figure 22. However, it is shown that the corresponding power dependent filtering effect was much weakened and exhibited a plateau pattern over a much broader power range, as the input signal wavelength was set farther away from the zero-dispersion wavelength value. The first power trough appeared at a much higher input signal power value. This might be attributed to the pulse broadening effect of the input signal in this normal dispersion regime and had led to reduced peak power of the input signal. Thus, SPM effect was much weakened. To alleviate this, input signal pulses with much narrower pulsewidth might be required. As a result, the input signal wavelength value should be chosen not too far away from the zero-dispersion wavelength in the normal dispersion regime to assure signal coherence as well as better power contrast in the power dependent filtering operation.

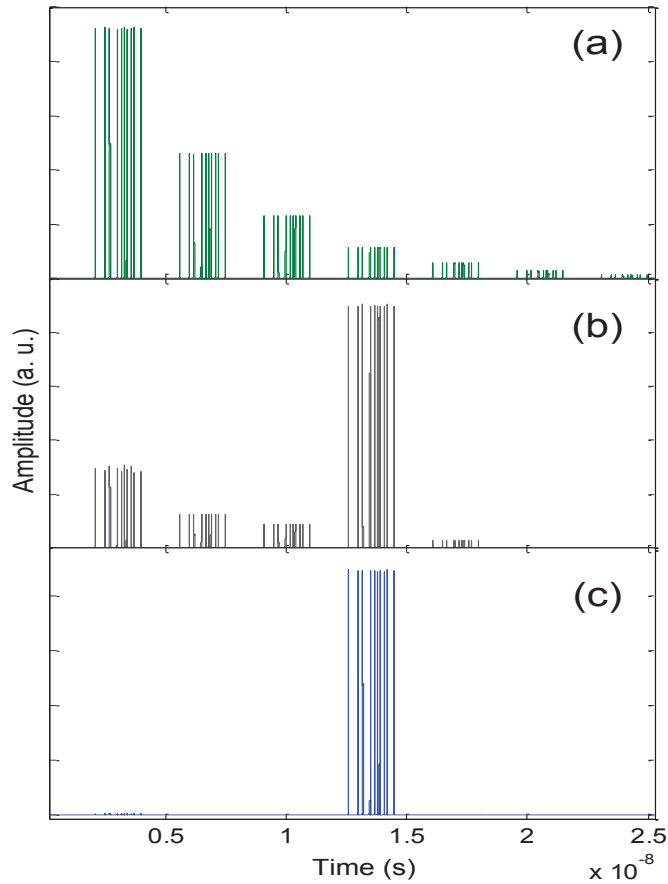


Figure 23 : Simulated outputs when the delay is controlled as 3 steps from its initial timing position. (a) The input packet train copies, (b) output from Stage 1, (c) output from Stage 2.

Figure 23(a)-(c) show the packet copies of the input signal, and the output signals of Stages 1 and 2, respectively, when the input signal pulse was delayed by three steps from its initial position. Figure 24 shows the output signals of the optical packet buffer when the input signal pulses with different power levels were inputted. It is observed that the output pulse was delayed by one further step when the input signal power was subsequently amplified by every 3 dB more, via the delay control EDFA, in the setup. The input signal power at its initial timing position was taken as 0-dB gain at the EDFA, as a reference.

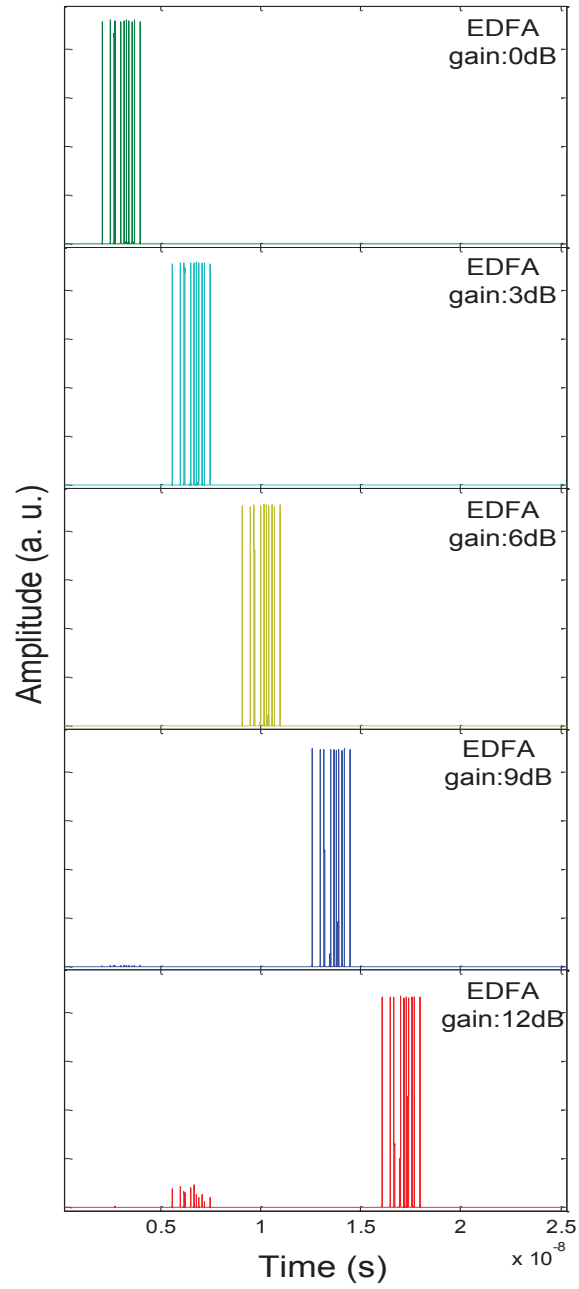


Figure 24 : Simulated outputs of optical packet buffer when the input signal is having different EDFA gains, which give different input signal power levels.

3.4 Experimental Results

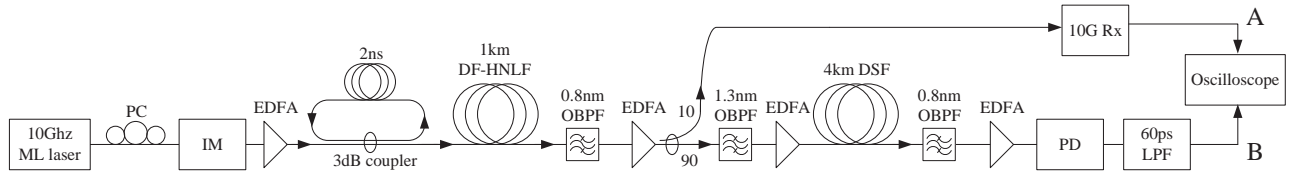


Figure 25 : Experimental setup. (PD: photodiode, LPF: low pass filter)

The proof-of-concept of the proposed optical packet buffer has been experimentally investigated with the setup depicted in Figure 25. The output of the semiconductor mode-locked laser at 1544.94 nm with 10-GHz 2-ps pulse train was modulated by an optical intensity modulator to gate an optical pulse for every 64 pulses. The output of the intensity modulator was then amplified by an EDFA before being fed into the passive optical circuit formed by a 3-dB coupler which introduced 2-ns delay difference, and 3-dB power difference between each consecutive copy. The signal was then fed into the first stage of SPM followed by offset filtering which was made up of a piece of 1-km DF-HNLF, having a nonlinear coefficient, zero dispersion wavelength and dispersion slope of $10.8 \text{ W}^{-1} \cdot \text{km}^{-1}$, 1550 nm and $0.007 \text{ ps}/(\text{nm}^2 \cdot \text{km})$, respectively. The parameters were the same as that adopted in the numerical simulation in section III. At the output of the HNLF, a 0.8-nm bandwidth OBPF centered at 1541 nm was used to slice the spectrally broadened signal. The spectrally sliced signal was then amplified before being fed into another piece of 4-km dispersion-shifted fiber (DSF) for power thresholding operation. At the output of the DSF, the signal was finally filtered out by another 0.8-nm OBPF at 1535.5 nm and was detected by a 50-

GHz photo-detector, followed by an electrical low-pass filter, in order to observe the delayed waveforms on the oscilloscope.

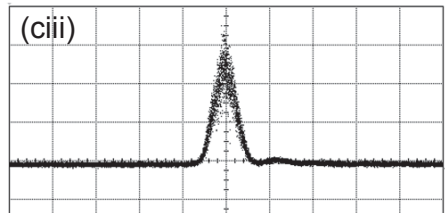
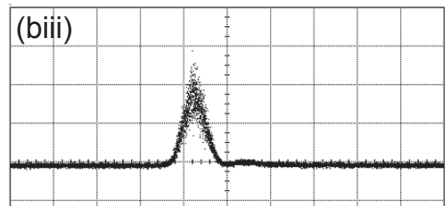
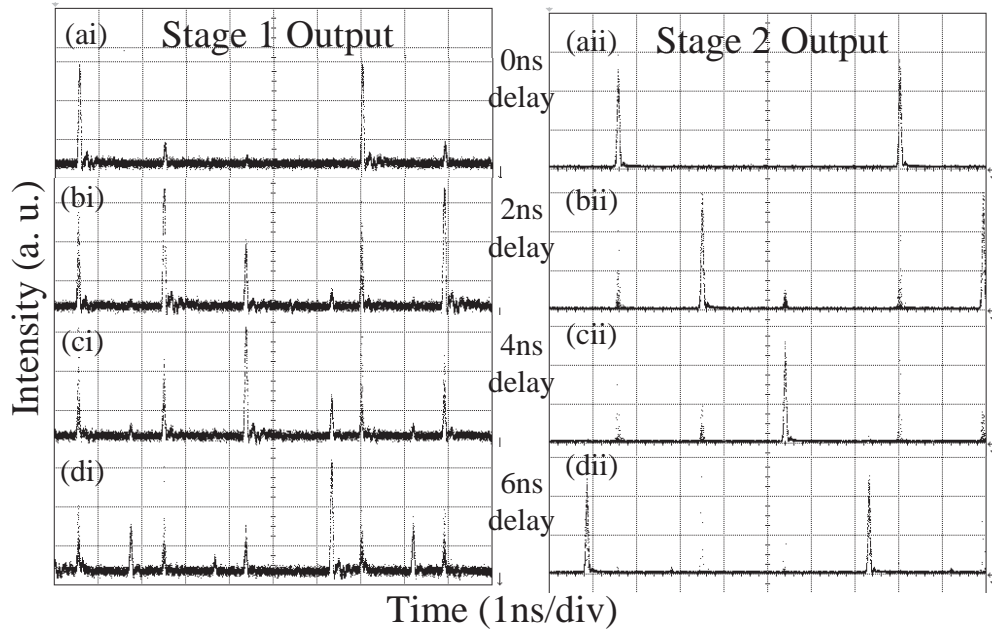


Figure 26 : (i) Stage 1 output at point A in Fig. 4, (ii) Stage 2 output at point B in Fig. 4 with different input signal power levels at Stage 1: (a) 0.4 dBm, (b) 3.85 dBm, (c) 6.25 dBm, (d) 8.75 dBm. (biii) & (ciii): enlarged traces at the output of Stage 2 of (bii) and (cii), respectively.

Figure 26 (a)-(d) show the outputs of the two stages when the input signal power level was varied. At the output of Stage 2, it was observed that the output signal was delayed by 0 ns, 2 ns, 4 ns and 6 ns, when their respective input signal power levels were 0.4 dBm, 3.85 dBm, 6.25 dBm and 8.75 dBm, in which the power difference between each consecutive delay was roughly 3 dB. The Stage 1 output showed the signal extinction ratio of about 3 dB while the Stage 2 output showed the improvement of the signal extinction ratio after power thresholding operation. The results confirm the proof-of-concept of the proposed optical packet buffer, though the experimental results can be further improved by using HNLF of higher nonlinear coefficient to enhance the SPM effect, as well as optimizing the system parameters, such as pulsewidth, wavelength and power of the input signal.

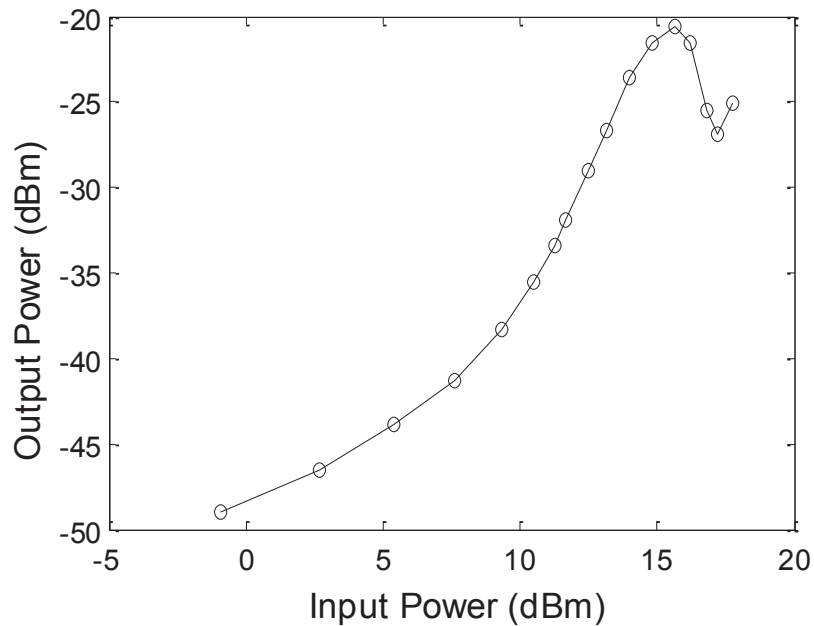


Figure 27 : The power transfer curve of Stage 1 output.

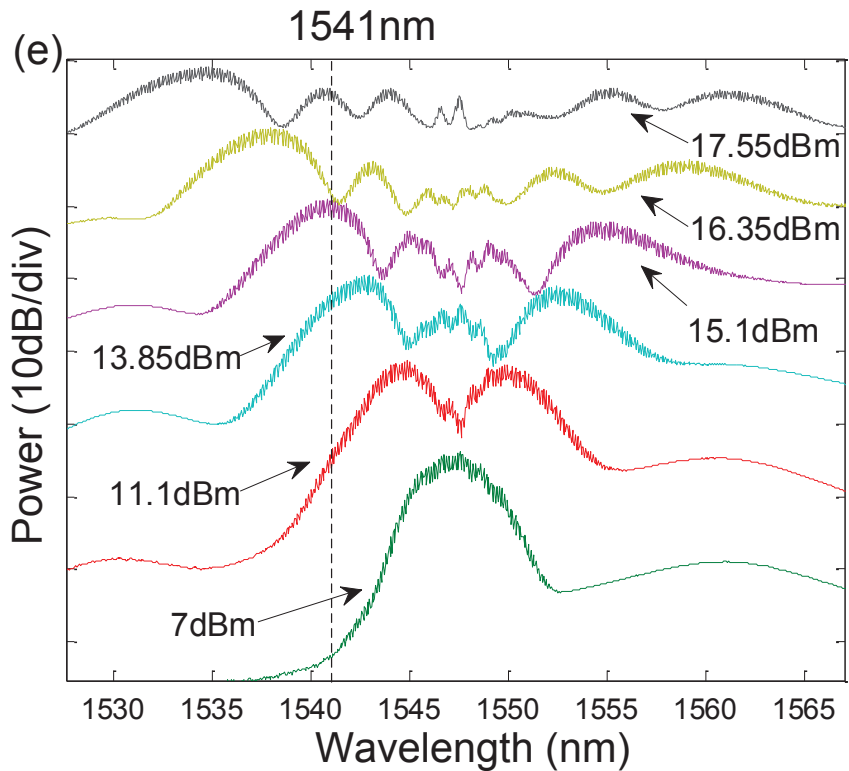


Figure 28 : the spectra evolution of the output pulse train at Stage 1 with different input power levels to the nonlinear fiber. (The spectra are arranged in the graph to avoid overlapping and the dotted line denotes the filter offset position at wavelength 1541nm)

Figure 27 shows the power transfer curve at Stage 1, showing the power dependent filtering phenomenon. Figure 28 shows the measured spectral evolution of the output pulse train at Stage 1 at different input signal power levels to the HNLF. When starting at low input power level, say 7 dBm, the output spectrum comprised only one spectral lobe centering at the input wavelength. Increasing the input signal power to 11.1 dBm would give rise to two spectral lobes in the spectrally broadened signal. Further increase in input power level to 13.85 dBm would form three spectral lobes in the spectrally broadened signal, and so on. Therefore, the spectral broadening increased when input signal power increased.

More importantly, it was observed that the outermost spectral sidelobes contained more power than the inner spectral lobes. The asymmetry of the broadened spectrum was attributed to the fiber chromatic dispersion. By setting the filter wavelength offset at 1541 nm, denoted as the dotted line in Figure 28, it was observed that the outermost spectral sidelobe fell into the passband of the offset filter when the input signal pulse stream was at 15.1 dBm and the outermost sidelobes were spread over wider wavelength range at higher input signal power level. Figure 27 shows the measured power transfer curve at the output of Stage 1 where the offset filter was centered at 1541 nm. The result confirmed that there was maximum output power when the input signal power was around 15 dBm.

3.5 Discussion

The optical power dependent filter of the proposed variable optical packet buffer can be implemented via two stages of SPM followed by offset filtering. The first stage extracts the outermost spectral sidelobe at the desired input signal power while the second stage performs power thresholding operation to further enhance the extinction ratio of the signal output. In addition to easy control of the delay by controlling the input signal power level, this scheme offers two features which are intrinsic to the SPM effect, namely polarization independent and no

additional laser source required. Besides, this scheme is potentially capable of supporting much higher bit rates.

In the current setup of the buffer, we employed a re-circulating loop implemented by a passive 3 dB coupler. It generated multiple copies of the input signal which were temporally spaced by a fixed time interval. The power of each delayed pulse copy was 3 dB lower than its previous one. We noticed that in order to realize longer delay, we should amplify the input signal at a larger gain. Owing to the 3-dB power relationship of the subsequent packet copies, for a packet to have n delay time steps in the buffer, its input power would be $n \times (3 \text{ dB})$ larger than the input signal power of the packet with minimal delay. However, from the numerically simulated power transfer curve of the Stage 2 output of the proposed optical packet buffer, as depicted in Figure 18, the output power was maximized when the input signal power level was about 15 dBm. Any 2-dB difference from this optimum input signal power level would lead to at least 20-dB reduction in the output power with respect to the maximum output power level. Therefore, the design of the proposed optical buffer can be further optimized in such a way that the power of each subsequent delayed packet copy from the passive optical delay loop circuit is 2-dB lower than its previous one. As a result, the proposed optical packet buffer can provide a larger number of delay steps with smaller range of input power control. Further study may be feasible in order to obtain an approximately ideal delta function in the power transfer profile of the buffer, which can further lower the input signal power range for different delay steps.

The power requirement of the system can be lowered if highly nonlinear optical fiber with higher nonlinear coefficient is employed. Recently, due to the advance of the development of highly nonlinear fiber, the nonlinear coefficient of the fiber can achieve beyond $1000 \text{ W}^{-1}\cdot\text{km}^{-1}$ by using highly nonlinear bismuth oxide fiber (Bi-NLF) [60], or photonic crystal fiber (PCF) [61]. As Bi-NLF and PCF can provide much higher nonlinear coefficient, the fiber length to be used inside the system can be much shortened, and the power requirement of the input signal can be much relaxed.

Regarding to the realization of the optical power dependent filtering operation in Stage 1, there may be other feasible approaches. For example, when the input pulse width is in femtosecond range and soliton self-frequency shifting (SSFS) [62] is utilized, the red wavelength shifted signal at the desired input signal power can be filtered out. The principle is similar to the case of SPM followed by offset filtering. As the increase in the input signal power level would lead to the increase in the red shifted wavelength offset of the signal, via SSFS, and vice versa. By setting the output filter at a certain strategic wavelength, there would be output power only at the specified input signal power and therefore realizes optical power dependent filtering operation. SSFS has been demonstrated to provide continuously tunable optical delay line [63], in which SSFS introduced input signal power dependent wavelength shift and in turn induced different time delays when the signal passed through a dispersive medium. However, long length of dispersive medium might be required in order

to obtain larger amount of time delay. Beside SSFS, triangular pulse or sawtooth pulse has been employed to perform all-optical wavelength conversion [64],[65]. Owing to the temporal profile of such special pulse shapes, through SPM or cross-phase modulation (XPM), the amount of wavelength shift would be intensity dependent, which thus can be a potential alternative approach to perform intensity dependent filtering in our proposed optical packet buffer with careful setting of the output filter wavelength. The generation of the triangular pulses can be realized through super-structured fiber Bragg grating technology [65] or chirped pulses propagating in a piece of normally dispersive fiber [66]. Regarding to the realization of the second stage which performs power thresholding operation, besides employing the Mamyshev regenerator structure, extinction ratio improvement can also be achieved through FWM [67], nonlinear amplifying optical loop mirror (NALM) [68],[69] or saturable absorber [70], etc..

3.6 Summary

We have proposed a novel all-fiber optical packet buffer in which the amount of induced time delay is easily controlled by changing the input signal power level. It is realized by employing a passive optical delay loop circuit, followed by two stages of SPM spectral broadening effect in HNLF with offset filtering. We have investigated and characterized the proposed variable all-

optical packet buffer both numerically and experimentally. Packet delay is achieved which can help to resolve the packet contention in future OPS systems.

Chapter 4 A Cost-effective Pilot-Tone-based Monitoring Technique for Power Saving in RSOA-based WDM-PON

In this chapter, we propose and experimentally demonstrate a simple and novel monitoring technique with the modulation of RSOA's ASE by the pilot-tone monitoring signal at the ONU, to facilitate power saving operation in RSOA-based WDM-PON. Our scheme can support the power-off operation of transceiver modules in OLT and ONU during power saving mode. In addition, power saving efficiency of this scheme is studied.

4.1 Introduction

Recently, there has been an increasing attention to power consumption saving in many fields. In information and communication technology (ICT), it is estimated that access network consumes around 70% of overall telecom network energy consumption [44] due to the presence of huge number of active devices. In addition, estimation shows that access networking equipments are less than 15% utilized [44] and large portion of energy is therefore consumed by the idle devices, as the networks are engineered for satisfying the peak traffic load requirement. Hence, reducing energy consumption in access networks can lead to major saving in Internet energy consumption.

There are some efforts on providing energy saving by allowing network elements to switch to sleep mode in time-division-multiplexed passive optical network (TDM-PON) [71], or wireless-optical broadband access network

(WOBAN) [44], etc. Beside TDM-PON, wavelength division multiplexing passive optical network (WDM-PON) is a promising solution for next generation broadband access architecture due to its large dedicated bandwidth for each subscriber. When the WDM-PON architecture is deployed in home or enterprise arenas, the optical network units (ONUs) may be idle for certain time period in a day, e.g. in the morning or at night. From [45], it was stated that the number of active network subscribers during the period between 0200 and 0800 are much less than that between 1700 and 2200. Moreover, WDM-PON can be integrated with wireless-mesh network as fiber-wireless (FiWi) architecture where multiple ONUs serve as gateways of a whole wireless-mesh network, similar to WOBAN which combines the advantages of both optical and wireless communications. Its multipath divergence characteristic of this architecture provides load balancing and failure restoration features. Therefore, the idle ONUs during off-peak hours can be switched off for power saving.

In WDM-PON, the centralized light source (CLS) is necessary such that a portion of the downstream signal power is re-modulated by the upstream data. Several re-modulation schemes have been proposed, including downstream differential phase shift keying (DPSK) and upstream on-off keying (OOK) [39], downstream frequency shift keying (FSK) and upstream OOK [72], etc. In the re-modulating WDM-PON architectures, re-modulation by a reflective semiconductor optical amplifier (RSOA) with OOK at the ONU is a promising solution [42] as it provides gain to the re-modulating signal and offers compactness and colorless properties to ONUs. However, the re-modulating

WDM-PON architectures suffer from a power consumption problem. Without the downstream signal, the ONU cannot send the upstream data. Thus even if there is no traffic on the line, the optical line terminal (OLT) has to send the downstream signal all the time. Therefore, when the ONU and the corresponding transceiver at OLT are in sleep mode for energy saving, some techniques have to be employed for the ONU to send “wake-up” message to OLT to request for initiating data transmission. The work in [46] proposed using polling scheme of a tunable supervisory transceiver, while [47] utilized light-emitting-diode (LED) based monitoring signal.

4.2 Proposed System Architecture

Figure 29 illustrates the proposed power-efficient WDM-PON architecture. At the OLT, all the downstream signals are wavelength-multiplexed by an arrayed waveguide grating (AWG) and transmitted to the remote node (RN) along the feeder fiber. At the RN, the downstream WDM signals are demultiplexed by an AWG and distributed to the corresponding destined ONU. At the ONU, half of the signal power is fed into an optical receiver to retrieve the downstream signal while another half is re-modulated by a RSOA by the upstream data. The upstream signal is then delivered to the OLT, via the AWG at the RN again and another feeder fiber to avoid possible Rayleigh backscattering.

instance, when there is an upstream data request from ONU N , the RSOA at ONU N will be modulated by an ONU-specific low frequency sinusoidal monitoring signal f_N . As there is no downstream signal, the RSOA is not injection-locked and its broadband ASE signal is modulated by the sinusoidal monitoring signal. It will then be spectral sliced by the AWG at the RN, as shown in Figure 30, such that only the wavelengths ($\lambda_{N,n}^M = \lambda_N + n\text{FSR}$, for $n=1, \dots$) are transmitted to the OLT, due to the cyclic spectral property of the AWG. At the OLT, one portion of the received monitoring signal is extracted by the R/B splitter and detected by a dedicated pilot-tone monitoring module. After detected by photodiode, Fast Fourier transform (FFT) will be performed on the detected electrical signal to examine if any specific pilot tone sent from any ONU is present. If yes, it will activate the respective transceiver at the OLT and returns to normal operation mode, which delivers the downstream signal power in continuous wave or with data.

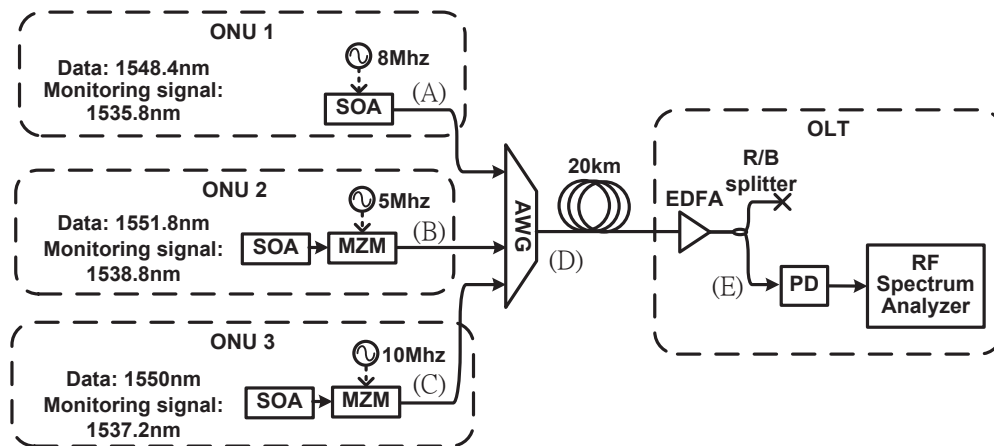


Figure 31 : Experimental setup. (SOA: semiconductor optical amplifier, MZM: Mach Zehnder Modulator, PD: photodetector)

4.3 Experimental Setup and Result

We demonstrated the feasibility of the proposed WDM-PON monitoring scheme based on the experimental setup, as shown in Figure 31. In the experiment, we only demonstrated the sending of the monitoring signal upstream and the detection of the pilot tones from all ONUs at OLT, because the monitoring scheme was non-intrusive to the in-service data transmission. As an example, we emulated that only ONU 1 sent “wake-up” message. The SOA at the ONU, which was used to enumerate the RSOA was directly modulated by an 8-MHz sinusoidal signal. The output signal from the SOA had 1.9-dBm power and the spectrum of the directly modulated SOA was shown in Figure 32(a). It was then spectrally sliced by an AWG and the output power was -21.1 dBm, with the spectrum shown in Figure 32(b). After passing through 20-km single-mode fiber (SMF), the signal was amplified by an EDFA followed by a R/B splitter, which extracted 1529.3 nm to 1542.39 nm range wavelengths at one output. The output power was -18.2 dBm, with the spectrum shown in Figure 32(c).

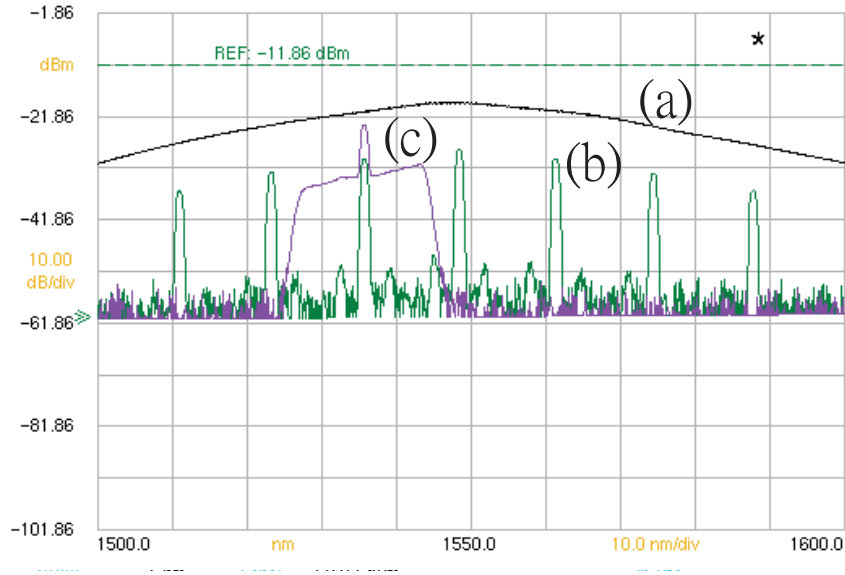


Figure 32 : (a) The spectrum of the SOA output at ONU1 (point A in Figure 31), (b) After AWG (point D in Figure 31), (c) After R/B splitter (point E in Figure 31)

In the experiment, due to the characteristic of R/B splitter employed, in order to allow the data channels to be occupied between 1545-60nm region, only monitoring signals at 1529.3 nm to 1542.39 nm were selected such that only one monitoring signal per one channel was detected. However, by using a filter which extracted the data channels from the monitoring signals, the monitoring signals of a channel at multiple wavelengths could be detected by the pilot-tone detector instead. After detection, via a photodiode, the electrical signal was then analyzed using an RF spectrum analyzer. The RF spectrum was shown in Figure 33 (a). It was observed that there existed higher-order harmonic frequency tones due to the imperfect modulation of the SOA with sinusoidal signal, though the power of the second-order harmonic frequency tone was 20-dB lower than that of the fundamental one. From Figure 32(c), it was observed that although the optical signal-to-noise ratio (OSNR) of the amplified signal was not very high,

due to the ASE noise of EDFA, there was still about 50-dB difference in power level between the pilot tone and the noise floor in the RF spectrum. This showed the superior performance of the proposed pilot-tone monitoring scheme under low OSNR condition. We then performed a multi-ONU monitoring experiment by adding two more ONUs, each comprised an SOA followed by an optical intensity modulator to emulate the RSOA. The optical modulators were driven by electrical sinusoidal signals at 5 MHz and 10 MHz, respectively. Due to the insertion loss of the optical modulators, the ONU2's output power at point B (denoted in Figure 31) was -2.25 dBm, while the ONU3's output power at point C was -5.9 dBm. Figure 33 (b)&(c) shows the RF spectra when ONU 1&2, and all three ONUs were sending "wake-up" message, respectively. Due to the lower-power of the monitoring signals of ONU2 and ONU3, their pilot-tone monitoring signals in the RF spectrum had lower power level than that of the ONU1.

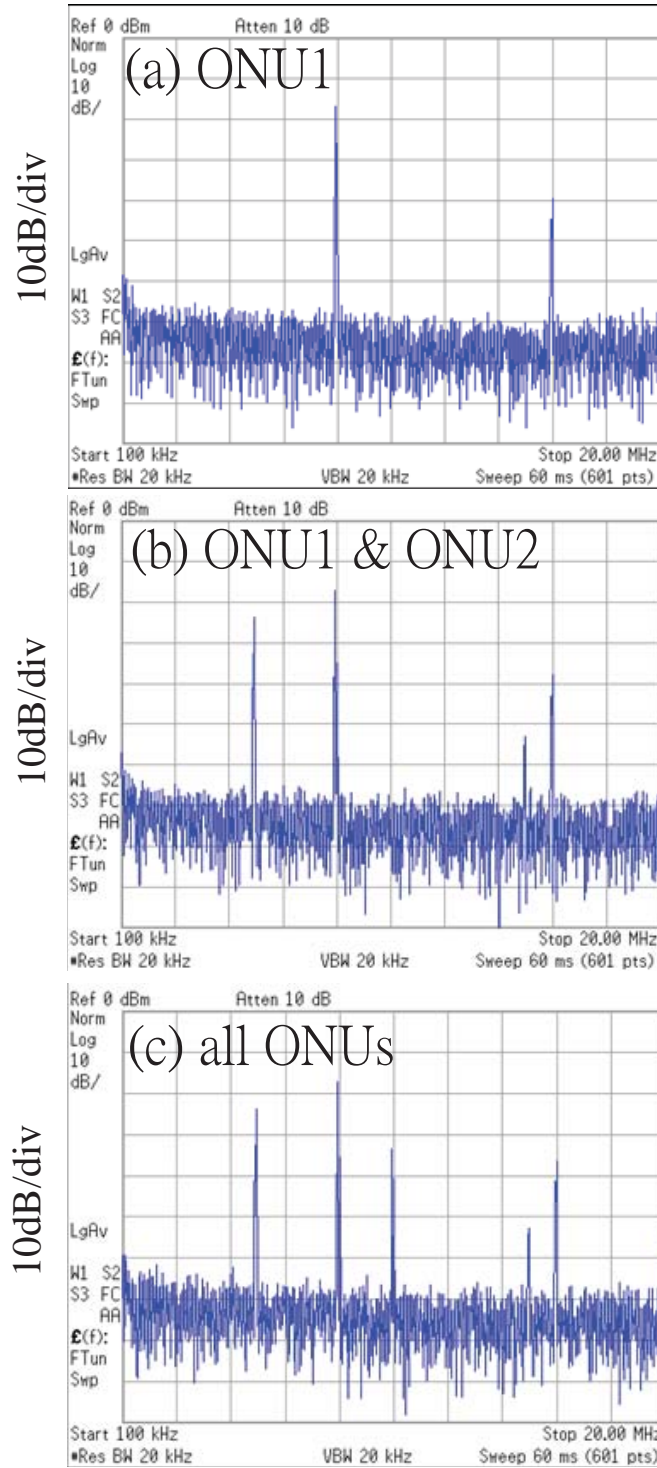


Figure 33 : RF spectrum of the detected signal with different ONU sending “wake-up” message(a) only ONU 1, (b) ONU1&ONU2, (c) all ONUs.

4.4 Power Saving Efficiency Calculation

Our proposed power saving scheme makes use of a dedicated monitoring module to monitor the “wake-up” requests from all power saving ONUs, therefore the transceivers of the corresponding ONUs at the OLT can be turned off to provide power saving feature at OLT.

To estimate the power saving efficiency of the proposed scheme, we have compared the ratio of amount of power required at the OLT provided by the proposed scheme with the conventional scheme that the transceivers at the OLT are activated continuously throughout the years. We have adopted similar analysis as in [46]. In our proposed scheme, the only additional power required at the OLT is the operating power for the dedicated monitoring module which consists of photodiode, FFT calculation circuit and simple control circuit. Although EDFA is employed to amplify the monitoring signals from all ONUs, it is also used for the signals’ amplification as well. The additional power required to amplify the monitoring signals at the EDFA is negligible as the input power of the monitoring signals is very small, as compared with the input data signals.

In the following calculation, we denote the ratio of power required by the dedicated monitoring module compared with a transceiver at the OLT as m . We consider it as in the range between 0.5 and 2. As a single monitoring module is shared by all ONUs, the impact of its additional power requirement decreases

when the number of the ONUs in the PON increases, hence makes our proposed scheme more efficient. The system power ratio of the proposed scheme to the conventional scheme is defined as

$$P_S = \frac{\text{Average power required of the proposed scheme}}{\text{Average power required of the conventional scheme}}$$

By considering the probability of ONUs entering sleep mode:

$$P_S = \sum_{k=0}^n C_k^n (1-t)^{n-k} t^k \left(\frac{n-k+m}{n} \right) \times 100\%$$

where the n is number of ONUs in the PON, k is the number of ONUs entering power saving mode at the same time, and t is the ratio of average power saving time of each channel at the OLT (e.g. $t=4/24$ represents the ONU have total 4 hours in power saving mode in the whole day). Ideally, if m takes the value of zero, system power ratio $P_S=(1-t)$. Figure 34 shows the system power ratio P_S versus different numbers of ONUs with different ratios of power saving time t . We can observe that when the number of ONUs reaches 32, the system power ratio will almost reach its optimal point (system power ratio $\rightarrow 1-t$ when the number of ONUs $\rightarrow \infty$). Figure 34 shows the system power ratio P_S versus different numbers of ONUs with different value of m . We can notice that with higher power required by the monitoring device, the system power ratio decreases more rapidly with the increase of the number of ONUs.

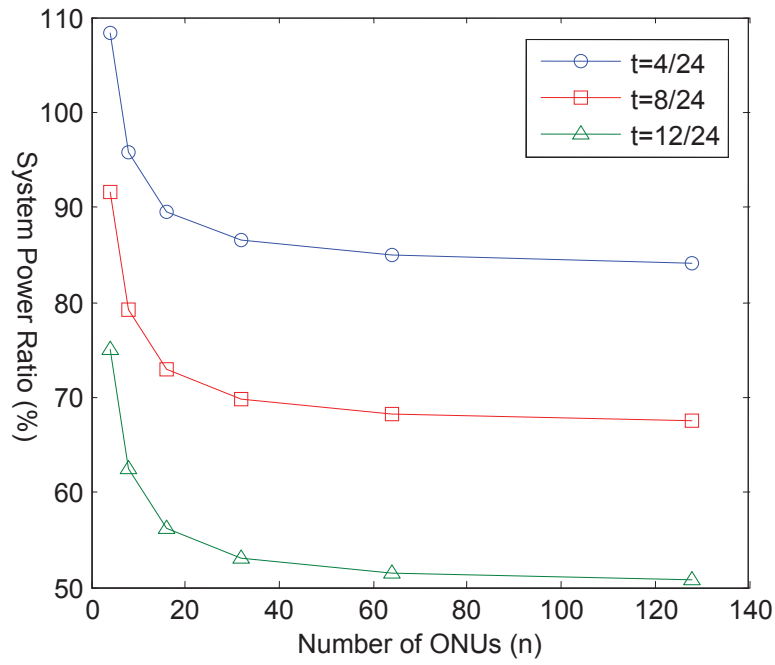


Figure 34 : System power ratio versus different numbers of ONUs with different ratios of power saving time.

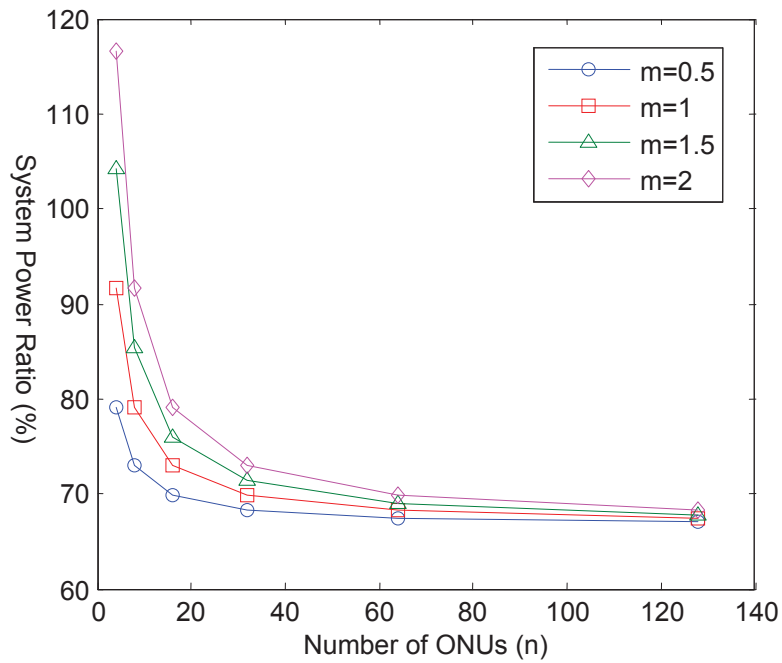


Figure 35 : System power ratio versus different numbers of ONUs with different powers required by the monitoring device.

In the above discussion, we have considered that each ONU in the PON can enter power saving mode randomly during the whole day. However, we can further model the behavior of the ONUs by taking into consideration that they just enter power saving mode during particular hours in each day. As a result, the dedicated monitoring device can be turned off when the ONUs are not likely to enter the power saving mode. The system power ratio calculation will be updated as

$$P_S = \left[\frac{h}{24} \sum_{k=0}^n C_k^n (1-t)^{n-k} t^k \left(\frac{n-k+m}{n} \right) + \frac{24-h}{24} \right] \times 100\%$$

where h is the number of hours per day that the ONUs will enter power saving mode only during that period. Figure 36 shows the system power ratio P_S versus different numbers of ONUs with different power saving periods while having the same ratio of power saving time at each ONU. We can observe that when the ONU power saving mode occurs only in a smaller period, the system power ratio P_S will decrease and approach to the limit $(1-t)$ much further as the monitoring device can be turned off for longer time, therefore more power can be saved.

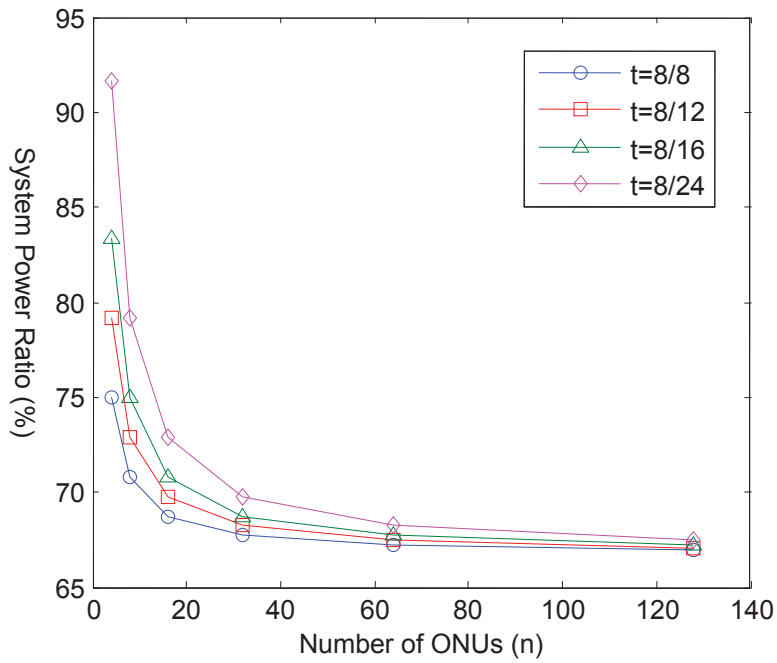


Figure 36 : System power ratio versus different numbers of ONUs with different power saving periods.

4.5 Summary

We have proposed a simple and cost-effective monitoring scheme using pilot tone-based monitoring signal in WDM-PON to provide power saving, by allowing the ONU and the corresponding transceiver at OLT to enter sleep mode during idle time. Feasibility of the scheme has been demonstrated through experiments.

Chapter 5 Conclusions and Future Work

5.1 Conclusions

We have proposed novel signal processing techniques to solve the crucial problems in all-optical networks, including lightpath tracing and packet contention resolution in all-optical packet switched network and energy saving in WDM-PON.

To perform lightpath tracing in all-optical packet switched network, each intermediate network node is assigned with a distinct prime number and we have proposed by the use of all-optical label encoders in the intermediate network nodes to perform label tag prime number multiplication. At the receiver, the route information is contained at the final label value which is the product of the prime number label tags of the traversed nodes. Through factorization of the label value at the destination node, we can retrieve the list of intermediate nodes that the packet has traversed.

For solving the contention problem in all-optical packet switched network, we have proposed a novel all-optical variable packet buffer which the packet delay can be controlled through varying the input signal power. The larger the input signal power, the longer the packet delay is. The all-optical variable packet buffer consists of fiber re-circulating circuit and two stages of SPM in HNLF followed by offset filtering.

In order to allow energy saving operation in WDM-PON employing upstream re-modulation technique, we have proposed a novel signal processing technique to send wake-up message when the corresponding transceiver module at the OLT is turned off. At the ONU, by modulating the RSOA's ASE with a distinct pilot tone frequency, the dedicated monitoring module at the OLT can detect the sum of all ONUs' wake-up pilot tone signals and extract the corresponding ONUs sending those signals. The OLT can then activate the corresponding ONUs' transceivers for data transmission.

5.2 Future Work

In lightpath tracing scheme in all-optical packet switched network, we have proposed a mechanism to perform lightpath tracing using prime number multiplication and we suggest the label receiver to be placed at the packet drop port. However, we can also detect the labels of the packets at the intermediate nodes so as to perform more strategic lightpath monitoring. For example, we can place the label monitors at the network nodes which are heavily loaded such that the majority of the packets' route information can be detected and the route information can be more centralized for the convenient of further computing. The route information captured by those label monitors should be able to retrieve the crucial information of the network status that can favor fault monitoring, QoS assurance, etc. In such situation, studies should be performed in order to decide

the placement of the label monitors in the network. Similar to the above discussion, in [73], we have proposed a novel fault detection and localization scheme for all-optical networks with the path information of real-time data traffic and studied the placement of the label monitors in k -shortest paths routing network with $k=2$. Our adaptive fault localization framework is based on combining passive and proactive monitoring solutions, together with adaptive management in two phases.

In addition, further demonstrations should be held to manufacture the all-optical label encoder with PLC technology in order to realize a more compact device for system integration.

In the all-optical variable packet buffer, further studies should be performed to realize it with wavelength preservation capability. It can be realized in our proposed structure when the center wavelength of the optical filter after the second stage of SPM is set to the input signal's wavelength. However, careful studies are needed for the nonlinear fibers used and the filters' bandwidth in order to obtain desirable power dependent filtering operation.

In the signaling technique to support energy saving operation in WDM-PON with upstream re-modulation, system prototype is needed to demonstrate the pilot tone detection speed of the monitoring module which governs the wake-up delay experienced by the ONUs.

Bibliography

- [1] M. Ilyas and H. T. Mouftah, “The handbook of optical communication networks,” *CRC Press*, 2003.
- [2] S. Yao, S. Dixit and B. Mukherjee, “Advances in photonic packet switching: an overview,” *IEEE Commun. Mag.*, vol. 38, no. 2, pp. 84–94, Feb. 2000.
- [3] J. E. Sharping, Y. Okawachi, J. van Howe, C. Xu, Y. Wang, A. E. Willner, and A. L. Gaeta, “All-optical, wavelength and bandwidth preserving, pulse delay based on parametric wavelength conversion and dispersion,” *OSA Opt. Exp.*, vol. 13, no. 20, pp. 7872–7877, Oct. 2005.
- [4] N. Alic, J. R. Windmiller, J. B. Coles, and S. Radic, “Two-pump parametric optical delays,” *IEEE J. Sel. Topics Quantum Electron.*, vol. 14, no. 3, pp. 681–690, May/Jun. 2008.
- [5] J. L. Corral, J. Marti, J. M. Fuster, and R. I. Laming, “True time-delay scheme for feeding optically controlled phased-array antennas using chirped-fiber gratings,” *IEEE Photon. Technol. Lett.*, vol. 9, no. 11, pp. 1529–1531, Nov. 1997.
- [6] H. Shahoei, M. Li and J. Yao, “Continuously Tunable Time Delay Using an Optically Pumped Linear Chirped Fiber Bragg Grating,” *J. Lightw. Technol.*, vol. 29, no. 10, pp. 1465–1472, May. 2011.
- [7] M. Pisco, S. Campopiano, A. Cutolo and A. Cusano, “Continuously variable optical delay line based on a chirped fiber bragg grating,” *IEEE Photon. Technol. Lett.*, vol. 18, no. 24, pp. 2551–2553, Dec 2006.
- [8] J. D. LeGrange, J. E. Simsarian, P. Bernasconi, L. Buhl, J. Gripp, and D. T. Neilson, “Demonstration of an integrated buffer for an all-optical packet router,” *IEEE Photon. Technol. Lett.*, vol. 21, no. 12, pp. 781–783, Jun. 2009.
- [9] Z. Zhu, A. M. C. Dawes, D. J. Gauthier, L. Zhang, and A. E. Willner, “Broadband SBS slow light in an optical fiber,” *J. Lightw. Technol.*, vol. 25, no. 1, pp. 201–206, Jan. 2007.
- [10] A. E. Willner, B. Zhang, L. Zhang, L. Yan, and I. Fazal, “Optical signal processing using tunable delay elements based on slow light,” *IEEE J. Sel. Topics Quantum Electron.*, vol. 14, no. 3, pp. 691–705, May/Jun. 2008.

- [11] J. E. Sharping, Y. Okawachi, and A. L. Gaeta, "Wide bandwidth slow light using a Raman fiber amplifier," *Opt. Express*, vol. 13, no. 16, pp. 6092–6098, Aug. 2005.
- [12] D. Dahan and G. Eisenstein, "Tunable all optical delay via slow and fast light propagation in a Raman assisted fiber optical parametric amplifier: a route to all optical buffering," *Opt. Express*, vol. 13, no. 16, pp. 6234–6249, Aug. 2005.
- [13] A. M. Liu, C. Q. Wu, M. S. Lim, Y. D. Gong, and P. Shum, "Optical buffer configuration based on a 3×3 collinear fibre coupler," *IET Electron. Lett.*, vol. 40, no. 16, pp. 1017–1019, Aug. 2004.
- [14] R. Langenhorst, M. Eiselt, W. Pieper, G. Grosskopf, R. Ludwig, L. Kuller, E. Dietrich, and H. G. Weber, "Fiber loop optical buffer," *J. Lightw. Technol.*, vol. 14, no. 3, pp. 324–335, Mar. 1996.
- [15] E. F. Burmeister, J. P. Mack, H. N. Poulsen, B. Stamenic, M. Masanovic, D. J. Blumenthal, and J. E. Bowers, "Demonstration of contention resolution between two 40 Gb/s packet streams using multiple photonic chip optical buffers," *European Conference on Optical Communication (ECOC), Brussels, Belgium, 2008, Paper We.2.D.3*.
- [16] M. Cheng, C. Wu, J. Hiltunen, Y. Wang, Q. Wang, and R. Myllyla, "A variable delay optical buffer based on nonlinear polarization rotation in semiconductor optical amplifier," *IEEE Photon. Technol. Lett.*, vol. 21, no. 24, pp. 1885–1887, Dec. 2009.
- [17] Y. Liu, M. T. Hill, R. Geldenhuys, N. Calabretta, H. de Waardt, G. D. Khoe, and H. J. S. Dorren, "Demonstration of a variable optical delay for a recirculating buffer by using all-optical signal processing," *IEEE Photon. Technol. Lett.*, vol. 16, no. 7, pp. 1748–1750, Jul. 2004.
- [18] T. Sakamoto, K. Noguchi, R. Sato, A. Okada, Y. Sakai, and M. Matsuoka, "Variable optical delay circuit using wavelength converters," *IET Electron. Lett.*, vol. 31, no. 7, pp. 454–455, Mar. 2001.
- [19] V. A. Vaishampayan and M. D. Feuer, "An overlay architecture for managing lightpaths in optically routed networks," *IEEE Transactions on Communications*, vol. 53, no. 10, Oct. 2005.
- [20] R. Rejeb, M. S. Leeson, and R. J. Green, "Fault and attack management in all-optical networks," *IEEE Commun. Mag.*, vol. 44, no. 11, pp. 79–86, Nov. 2006.

- [21] E. Kong, F. Tong, K. P. Ho, L. K. Chen, and C. K. Chan, "Pilot-tone based optical-path supervisory scheme for optical cross-connects," *Electron. Lett.*, vol. 35, no. 17, pp. 1481-1483, 1999.
- [22] S. Zhong, W. Chen, X.-H. Yang, and Y.-J. Chen, "Transparent optical path and crosstalk monitoring scheme for arrayed waveguide grating-based optical cross connect," *IEEE Photon. Technol. Lett.*, vol. 12, no. 9, pp. 1249-1251, Sept. 2000.
- [23] C. C. Lee, T. C. Kao, H. C. Chien, and S. Chi, "A novel supervisory scheme for OXC based on different time-delay recognition," *IEEE Photon. Technol. Lett.*, vol. 17, no. 12, pp. 2745-2747, Dec. 2005.
- [24] J. Yu, L. K. Chen, G.-W. Lu, and S.-T. Ho, "An improved OXC supervisory scheme based on different time-delay recognition," *Joint International Conference on Optical Internet and Next Generation Network (COIN-NGNCON)*, Paper PS-13, Jeju, Korea, Jul. 2006.
- [25] Z. Qian, G. W. Lu, and S.-Y. Li, "Efficient OXC monitoring based on time-delay recognition," *International Conference on Transparent Optical Networks (ICTON)*, Paper We.B3.4, Nottingham, United Kingdom, Jun. 2006.
- [26] Z. Qian, G. W. Lu, and S.-Y. Li, "Improved optical-path supervisory scheme for optical cross connects based on different time-delay recognition," *OSA J. Opt. Netw.*, vol. 7, no. 1, pp. 80-87, Jan. 2008.
- [27] S. Matsuoka, Y. Yamabayashi, K. Aida, and K. Nakagawa, "Supervisory signal transmission methods for optical amplifier repeater system," *GLOBECOM '90 vol.3*, pp 1846-1850, 1990.
- [28] H. S. Chung, S. K. Shin, K. J. Park, H. G. Woo, and Y. C. Chung, "Effects of Stimulated Raman Scattering on Pilot-Tone-Based WDM Supervisory Technique," *IEEE Photon. Technol. Lett.*, vol.12, no. 6, pp 731-733, June 2000.
- [29] J. J. Vegas Olmos, I. Tafur Monroy, A. M. J. Koonen and Yonglin Y, "High bit-rate combined FSK/IM modulated optical signal generation by using GCSR tunable laser sources," *Optics Express*, Vol. 11, No. 23, pp. 3136-3140, Nov. 2003.

- [30] T. Kawanishi, K. Higuma, T. Fujita, J. Ichikawa, T. Sakamoto, S. Shinada and M. Izutsu, "High-Speed Optical FSK Modulator for Optical Packet Labeling," *Journal of Lightwave Technology*, vol. 23, no. 1, pp. 87-94, Jan 2005.
- [31] T. Tanimura, T. Hoshida, S. Oda, Y. Akiyama, H. Nakashima, Y. Aoki, Y. Cao, M. Yan, Z. Tao, and J. C. Rasmussen, "Superimposition and Detection of Frequency Modulated Tone for Light Path Tracing Employing Digital Signal Processing and Optical Filter," *OFC/NFOEC2011, paper OW4G4, Los Angeles, California, USA, 2011*.
- [32] V. A. Vaishampayan, and M. D. Feuer, "An overlay architecture for managing lightpath in optically routed networks," *IEEE Trans. Commun.*, vol. 53, no. 10, pp. 1729-1737, Oct. 2005.
- [33] M. D. Feuer, and V. A. Vaishampayan, "Rejection of interlabel crosstalk in a digital lightpath labeling system with low-cost all-wavelength receivers," *IEEE/OSA J. Lightwave Technol.*, vol. 24, no. 3, pp. 1121-1128, Mar. 2006.
- [34] T. Ohara and M. D. Feuer, "Demonstration of lightpath labeling technique for multi-channel DPSK signals," *OFC/NFOEC2009, paper JWA46, San Diego, California, USA, 2009*
- [35] M. D. Feuer, V. A. Vaishampayan, V. Mikhailov, and P. Westbrook, "Digital lightpath label transcoding for dual-polarization QPSK systems," *OFC/NFOEC2011, paper JWA28, Los Angeles, California, USA, 2011*.
- [36] W. Wei, M. D. Feuer, D. Qian, P. N. Ji, N. Cvijetic, C. Wang and T. Wang, "A novel lightlabel orthogonal frequency division multiplexing (LL-OFDM) system for cross-layer lightpath monitoring and setup," *OFC/NFOEC 2009, paper PDPA7, San Diego, California, USA, 2009*.
- [37] C. F. Lam, "Passive optical networks: principles and practice," *Elsevier/Academic Press, 2007*.
- [38] L. Y. Chan, C. K. Chan, D. T. K. Tong, F. Tong, and L. K. Chen, "Upstream traffic transmitter using injection-locked Fabry-Perot laser diode as modulator for WDM access networks," *Electron. Lett.*, vol. 38, pp. 43-45, 2002.

- [39] W. Hung, C. K. Chan, L. K. Chen, and F. Tong, "An optical network unit for WDM access networks with downstream DPSK and upstream remodulated OOK data using injection-locked FP laser," *IEEE Photon. Technol. Lett.*, vol. 15, pp. 1476-1478, 2003.
- [40] G. W. Lu, N. Deng, C. K. Chan, and L. K. Chen, "Use of downstream IRZ signal for upstream data re-modulation in a WDM passive network," *Proc. OFC, 2005, Paper OF18*.
- [41] J. Zhao, L. K. Chen, C. K. Chan, "A novel re-modulation scheme to achieve colorless high-speed WDM-PON with enhanced tolerance to chromatic dispersion and re-modulation misalignment," *Proc. OFC, 2007, Paper OWD2*.
- [42] C. H. Wang, F. Y. Shih, C. W. Chow, C. H. Yeh, and S. Chi, "Using downstream DPSK signal for upstream OOK signal re-modulation with RSOA in hybrid WDM-TDM passive optical network," *OFC/NFOEC 2009*.
- [43] K. Y. Cho, Y. Takushima, and Y. C. Chung, "10-Gb/s operation of RSOA for WDM PON," *IEEE Photon. Technol. Lett.*, vol. 20, pp. 1533-1535, 2008.
- [44] P. Chowdhury, M. Tornatore, S. Sarkar and B. Mukherjee, "Building a Green Wireless-Optical Broadband Access Network (WOBAN)," *Journal of Lightwave Technology*, 2010.
- [45] <http://www.sandvine.com/downloads/documents/2009%20Global%20Broadband%20Phenomena%20-%20Executive%20Summary.pdf>
- [46] T. Uchikata and A. Tajima, "A novel power saving scheme for WDM-PON with centralized light sources." *OECC 2009, Paper TuH6*.
- [47] W. Jia, D. Shen, K.H. Tse, J. Xu, M. Li and C.K. Chan, "A Novel Scheme to realize a Power-efficient WDM Passive Optical Network," *OptoElectronics and Communications Conference (OECC) 2010, Paper 8A3-4, Sapporo, Hokkaido, Japan, Jul. 2010*.
- [48] K. Y. Liou, U. Koren, E. C. Burrows, J. L. Zyskind, and K. Dreyer, "A WDM access system architecture based on spectral slicing of an amplified LED and delay-line multiplexing and encoding of eight wavelength channels for 64 subscribers," *IEEE Photon. Technol. Lett.*, vol. 9, no. 4, pp. 517-518, Apr. 1997.
- [49] M.S. Rasras, et al, "A programmable 8-bit optical correlator filter for optical bit pattern recognition," *IEEE Photon. Technol. Lett.*, vol. 20, no. 9, pp. 694 - 696, May. 2008.

- [50] <http://www.samsungfiberoptics.com/En/Product/fttx09.pdf>
- [51] J. Armstrong, "OFDM for optical communication," *IEEE/OSA J. Lightwave Technol.*, vol. 27, no. 3, pp. 189-204, Feb. 2009.
- [52] P.V. Mamyshev, "All-optical data regeneration based on self-phase modulation effect," *ECOC 1998, Madrid, Spain*, pp. 475-476.
- [53] M. Matsumoto, Y. Shimada, and H. Sakaguchi, "Two-stage SPM-based all-optical 2R regeneration by bidirectional use of a highly nonlinear fiber," *IEEE J. Quantum Electron.*, vol. 45, no. 1, pp. 51-58, Jan. 2009.
- [54] J. Fatome and C. Finot, "Scaling guidelines of a soliton-based power limiter for 2R-optical regeneration applications," *IEEE/OSA J. Lightwave Technol.*, vol. 28, no. 17, pp. 2552-2559, Sept. 2010
- [55] S. H. Chung, X. Tang, and J. C. Cartledge, "Performance of a polarization-insensitive all-optical 3R regenerator using cross- and self-phase modulation and offset filtering in a recirculating loop," *OFC/NFOEC 2009, San Diego, CA, USA, paper OThF2*.
- [56] G. P. Agrawal, "Nonlinear Fiber Optics," *Academic Press*, 2001.
- [57] M. Nakazawa, H. Kubota and K. Tamura, "Random evolution and coherence degradation of a high-order optical soliton train in the presence of noise," *OSA Opt. Lett.*, vol. 24, no. 5, pp. 318-320, Mar. 1999.
- [58] Z. Yusoff, P. Petropoulos, K. Furusawa, T. M. Monro and D. J. Richardson, "A 36-channel x 10-GHz spectrally sliced pulse source based on supercontinuum generation in normally dispersive highly nonlinear holey fiber," *IEEE Photon. Technol. Lett.*, vol. 15, no. 12, Dec. 2003.
- [59] M. Nakazawa, K. Tamura, H. Kubota and E. Yoshida, "Coherence degradation in the process of supercontinuum generation in an optical fiber," *Optical Fiber Technology*, vol. 4, pp. 215-223, 1998.
- [60] M. P. Fok, and C. Shu, "Recent advances in optical processing techniques using highly nonlinear bismuth oxide fiber," *IEEE. Selected Topics Quantum Electron.*, vol. 14, no. 3, pp. 587-598, May/June 2008.

- [61] J. H. Lee, W. Belardi, K. Furusawa, P. Petropoulos, Z. Yusoff, T. M. Monro, and D. J. Richardson, "Four-wave mixing based, 10Gbit/s tunable wavelength conversion using a holey fiber with a high SBS threshold," *IEEE Photon. Technol. Lett.*, vol. 15, pp. 440-442, 2003.
- [62] F. M. Mitschke and L. F. Mollenauer, "Discovery of the soliton self-frequency shift," *OSA Opt. Lett.*, vol. 11, no. 10, pp. 659-661, 1986.
- [63] S. Oda and A. Maruta, "Experimental demonstration of all-optical tunable delay line based on soliton self-frequency shift and filtering supercontinuum spectrum," *ECOC 2006, Cannes, France*.
- [64] A. I. Lakin, S. Boscolo, R. S. Bhambher and S. K. Turitsyn, "Optical frequency conversion, pulse compression and signal copying using triangular pulses," *ECOC 2008, Brussels, Belgium, paper Mo.3.F.4*.
- [65] F. Parmigiani, M. Ibsen, T.T. Ng, L. Provost, P. Petropoulos and D. J. Richardson, "Efficient wavelength conversion using triangular pulses generated using a superstructured fiber Bragg grating," *OFC/NFOEC 2008, San Diego, CA, USA, paper OMP3*.
- [66] A. I. Latkin, S. Boscolo and S. K. Turitsyn, "Passive nonlinear pulse shaping in normally dispersive fiber," *OFC/NFOEC 2008, San Diego, CA, USA, paper OTuB7*.
- [67] A. Argyris, H. Simos, A. Ikiades, E. Roditi, and D., Syvridis, "Extinction ratio improvement by four-wave mixing in dispersion- shifted fibre," *Electron. Lett.*, vol. 39, no. 2, pp. 230-232, Aug. 2003.
- [68] A. G. Striegler and B. Schmauss, "Extinction ratio improvement by an advanced NOLM setup," *IEEE Photon. Technol. Lett.*, vol. 18, no. 9, May. 2006.
- [69] C. Stephan, K. Sponsel, G. Onishchukov, B. Schmauss, and G. Leuchs, "Phase-preserving amplitude regeneration in DPSK transmission systems using a nonlinear amplifying loop mirror," *IEEE J. Quantum Electron.*, vol. 45, no. 11, pp. 1336-1343, Nov. 2009.
- [70] D. Massoubre, J. L. Oudar, J. Fatome, S. Pitois, G. Millot, J. Decobert, and J. Landreau, "All-optical extinction-ratio enhancement of a 160 GHz pulse train by a saturable-absorber vertical microcavity," *Opt. Lett.*, vol. 31, no. 4, pp. 537-539, Feb. 2006.

- [71] S.-W. Wong, L. Valcarenghi, S.-H. Yen, D. R. Campelo, S. Yamashita and L. Kazovsky, "Sleep Mode for Energy Saving PONs: Advantages and Drawbacks," *GLOBECOM*, 2009.
- [72] N. Deng, W. Hung, C.K. Chan, L.K. Chen and F. Tong, "A novel wavelength modulated transmitter and its application in WDM passive optical networks," *OFC*, 2004.
- [73] D. Shen, K.H. Tse and C.K. Chan, "Adaptive Fault Monitoring in All-Optical Networks Utilizing Real-Time Data Traffic," *Journal of Network and Systems Management*, vol. 20, no. 1, pp. 76 - 96, Feb. 2012.

Publications during PhD Study

Journals:

- [1] **K.H. Tse** and C.K. Chan, "A Path Tracing Scheme for All-Optical Packet-Switched Networks," *IEEE OSA Journal of Lightwave Technology*, vol. 30, no. 6, pp. 1625-1631, Jun. 2012.
- [2] **K.H. Tse** and C.K. Chan, "A Novel Fiber-based Variable All-Optical Packet Buffer based on Self-Phase Modulation Induced Spectral Broadening," *IEEE Journal of Selected Topics in Quantum Electronics*, vol. 18, no. 2, pp. 654-661, Mar./Apr. 2012.
- [3] D. Shen, **K.H. Tse** and C.K. Chan, "Adaptive Fault Monitoring in All-Optical Networks Utilizing Real-Time Data Traffic," *Journal of Network and Systems Management*, vol. 20, no. 1, pp. 76 - 96, Feb. 2012.
- [4] W. Jia, J. Xu, Z.X. Liu, **K.H. Tse** and C.K. Chan, "Generation and Transmission of 10-Gb/s RZ-DPSK Signals using a Directly Modulated Chirp Managed Laser," *IEEE Photonics Technology Letters*, vol. 23, no. 3, pp. 173-175, Feb. 2011.

Conferences:

- [1] C.K. Chan and **K.H. Tse**, "Novel Optical Techniques for Lightpath Tracing and Monitoring in All-optical Reconfigurable Wavelength Routing Networks," *International Conference on Optical Communications and Networks, ICOCN 2011, (Invited Paper), Guangzhou, PRC, 2011.*
- [2] **K.H. Tse**, W. Jia and C.K. Chan, "A Cost-effective Pilot-Tone-based Monitoring Technique for Power Saving in RSOA-based WDM-PON," *IEEE/OSA Optical Fiber Communication Conference / National Fiber Optic Engineers Conference, OFC/NFOEC 2011, Paper OThB6, Los Angeles, California, USA, 2011.*
- [3] W. Jia, D. Shen, **K.H. Tse**, J. Xu, M. Li and C.K. Chan, "A Novel Scheme to realize a Power-efficient WDM Passive Optical Network," *OptoElectronics and Communications Conference, OECC 2010, Paper 8A3-4, Sapporo, Hokkaido, Japan, Jul. 2010.*

- [4] **K.H. Tse** and C.K. Chan, "A Novel Optical Encoding Scheme for Network Node Tracing in All-Optical Reconfigurable Wavelength Routing Networks," *European Conference on Optical Communications, ECOC 2009, Paper P5.02, Vienna, Austria, Sep. 2009.*